

## Photochemistry

## Exploring the Potential of Fulvalene Dimetals as Platforms for Molecular Solar Thermal Energy Storage: Computations, Syntheses, Structures, Kinetics, and Catalysis

Karl Börjesson,<sup>[a]</sup> Dušan Čoso,<sup>[b]</sup> Victor Gray,<sup>[a]</sup> Jeffrey C. Grossman,<sup>[c]</sup> Jingqi Guan,<sup>[d, e]</sup> Charles B. Harris,<sup>[d]</sup> Norbert Hertkorn,<sup>[d, f]</sup> Zongrui Hou,<sup>[d]</sup> Yosuke Kanai,<sup>[g, k]</sup> Donghwa Lee,<sup>[g, k]</sup> Justin P. Lomont,<sup>[d]</sup> Arun Majumdar,<sup>[b, h]</sup> Steven K. Meier,<sup>[d]</sup> Kasper Moth-Poulsen,<sup>[a, d]</sup> Randy L. Myrabo,<sup>[d]</sup> Son C. Nguyen,<sup>[d]</sup> Rachel A. Segalman,<sup>[i]</sup> Varadharajan Srinivasan,<sup>[j]</sup> Willam B. Tolman,<sup>[d]</sup> Nikolai Vinokurov,<sup>[d]</sup> K. Peter C. Vollhardt,<sup>\*,[d]</sup> and Timothy W. Weidman<sup>[d]</sup>

*Dedicated to my (P.V.) friend, Professor Max Malacria on the occasion of his 65th birthday (despite his 33 year effort to catch up, I am still three years older than he is)*

**Abstract:** A study of the scope and limitations of varying the ligand framework around the dinuclear core of FvRu<sub>2</sub> in its function as a molecular solar thermal energy storage framework is presented. It includes DFT calculations probing the effect of substituents, other metals, and CO exchange for other ligands on  $\Delta H_{\text{storage}}$ . Experimentally, the system is shown to be robust in as much as it tolerates a number of variations, except for the identity of the metal and certain

substitution patterns. Failures include 1,1',3,3'-tetra-*tert*-butyl (4), 1,2,2',3'-tetraphenyl (9), diiron (28), diosmium (24), mixed iron-ruthenium (27), dimolybdenum (29), and ditungsten (30) derivatives. An extensive screen of potential catalysts for the thermal reversal identified AgNO<sub>3</sub>-SiO<sub>2</sub> as a good candidate, although catalyst decomposition remains a challenge.

## Introduction

An attractive option for the utilization of sunlight to power the planet is a "closed cycle" molecular system, in which photonic energy is stored in the form of a relatively more energetic isomer of a species, to be released on demand as heat by reorganization to the original structure.<sup>[1]</sup> Such a construct would

constitute the essence of a recyclable thermal battery. We have explored the fulvalene [bi(cyclopentadienyldiene) or Fv] dimetallic frame 1 in this capacity, as it undergoes photoconversion to stable 2, from which it is regenerated by thermal or catalytic means (Scheme 1).<sup>[2]</sup> These studies encompass the initial discovery of the system,<sup>[2k]</sup> a detailed exploration of the mechanisms by which each step proceeds,<sup>[2b,f,h,j]</sup> the scrutiny of the ef-

[a] Dr. K. Börjesson, V. Gray, Prof. Dr. K. Moth-Poulsen  
Department of Chemical and Biological Engineering  
Chalmers University of Technology, 41296 Gothenburg (Sweden)

[b] Dr. D. Čoso, Prof. Dr. A. Majumdar  
Department of Mechanical Engineering  
University of California at Berkeley, Berkeley, CA 94720-1740 (USA)

[c] Prof. Dr. J. C. Grossman  
Department of Materials Science and Engineering  
Massachusetts Institute of Technology, Cambridge, MA 02139 (USA)

[d] Prof. Dr. J. Guan, Prof. Dr. C. B. Harris, Dr. N. Hertkorn, Dr. Z. Hou,  
J. P. Lomont, Dr. S. K. Meier, Prof. Dr. K. Moth-Poulsen, Dr. R. L. Myrabo,  
S. C. Nguyen, Dr. W. B. Tolman, Dr. N. Vinokurov, Prof. Dr. K. P. C. Vollhardt,  
Dr. T. W. Weidman  
Department of Chemistry, University of California at Berkeley  
Berkeley, California 94720-1460 (USA)  
E-mail: kpcv@berkeley.edu

[e] Prof. Dr. J. Guan  
College of Chemistry, Jilin University, Changchun 130023 (PR China)

[f] Dr. N. Hertkorn  
Analytical Biogeochemistry, Helmholtz Zentrum München  
85764 Neuherberg (Germany)

[g] Prof. Dr. Y. Kanai, Dr. D. Lee  
Department of Chemistry, University of North Carolina at Chapel Hill  
Chapel Hill, NC 27599-3290 (USA)

[h] Prof. Dr. A. Majumdar  
Present address: Department of Mechanical Engineering  
Stanford University, Stanford, California 94305-3030 (USA)

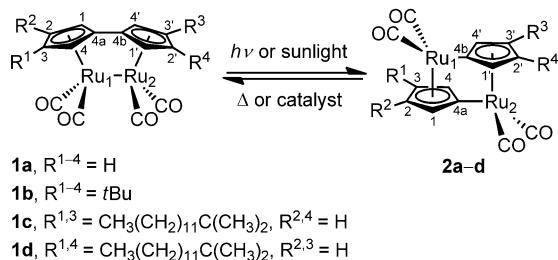
[i] Prof. Dr. R. A. Segalman  
Department of Chemical and Biomolecular Engineering  
University of California at Berkeley, Berkeley, CA 94720-1462 (USA)

[j] Prof. Dr. V. Srinivasan  
Department of Chemistry  
Indian Institute of Science Education and Research, Bhopal (India)

[k] Prof. Dr. Y. Kanai, Dr. D. Lee  
Condensed Matter and Materials Division  
Lawrence Livermore National Laboratory, Livermore, CA 94550 (USA)

Supporting information for this article is available on the WWW under <http://dx.doi.org/10.1002/chem.201404170>.

fects of varying the metal along the entire metal triad (Fe, Ru, Os), employing the relatively more soluble tetra-*tert*-butyl analogue (as in **1b** ⇌ **2b**),<sup>[2i]</sup> the behavior of the system when surface [Au(111)]-bound,<sup>[2g]</sup> the design and implementation of a device (featuring **1c,d** ⇌ **2c,d**),<sup>[2e]</sup> an assessment of the efficiency limit of such devices,<sup>[2d]</sup> an extension of the substituent scope to include fluoroalkyls,<sup>[2a]</sup> and the demonstration of photon upconversion with **1c,d** ⇌ **2c,d**.<sup>[2c]</sup>



Scheme 1. Photothermal cycle of the FvRu<sub>2</sub>(CO)<sub>4</sub> platform.

In the following narrative, we describe investigations outlining some of the scope and limitations of the system, comprising DFT calculations, syntheses, structural determinations, kinetics, thermodynamics, and the search for catalysts that facilitate the heat releasing step **2** → **1**.

## Results and Discussion

### DFT estimates

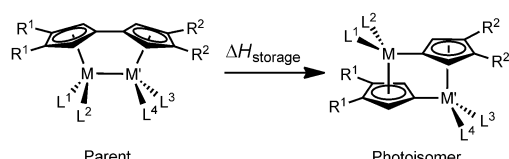
Differential scanning calorimetry of the conversion of **2a** to **1a** revealed that the former stores 19.8 kcal mol<sup>-1</sup>. Since the photoabsorption event generates excited **1a** at considerably higher energy (at λ<sub>max</sub> ~ 400 nm, > 70 kcal mol<sup>-1</sup>), calculational guidance was sought in the quest to design variously modified derivatives of FvRu<sub>2</sub>(CO)<sub>4</sub> with increased Δ*H*<sub>storage</sub> values. The results of a first screen in this respect, in which the placement of substituents on the Fv ligand is restricted to the unencumbered β- (relative to the Cp–Cp linkage, C<sub>4a</sub>–C<sub>4b</sub>; Cp = cyclopentadienyl), or 2- and 3-positions, are shown in Table 1.

Several data are noteworthy. To begin with, support for the accuracy of the computed numbers is provided by the measured values for **2a** → **1a** (19.8 kcal mol<sup>-1</sup>; cf. entry 1),<sup>[2h]</sup> **2b** → **1b** (vide infra, 21.1 kcal mol<sup>-1</sup>; cf. entry 3), and **2c,d** → **1c,d** (22.8 kcal mol<sup>-1</sup>; cf. related entries 3 and 4).<sup>[2e]</sup> In addition, selective comparison of the two computational methods [PBE/PW and BP86/LanL2dz&631+g(d,p)] reveals good agreement (entries 1, 2, 8, 9, 13, 15, and 26), the latter giving consistently slightly less positive numbers (≤ 1 kcal mol<sup>-1</sup>, except for entry 26, 2.3 kcal mol<sup>-1</sup>). As noted earlier for **1a** and **2a**,<sup>[2h]</sup> the topological features of those molecules for which X-ray structural analyses were performed (i.e., vide infra, **1b**, **2b**, **10**, **16**, **20**, and **21**) are reasonably reproduced in silico (see the Supporting Information). Focusing on the diruthenium system, tinkering with the fulvalene unit by 2,2',3,3'-substitution appears to have an only small effect (± ~ 2 kcal mol<sup>-1</sup>) on Δ*H*<sub>storage</sub>, elec-

tron pushers marginally increasing it (e.g., entries 2–5), acceptors decreasing it (e.g., entries 6–8). Benzofusion (indenyl) has no consequence (entries 9 and 10). Mixed push–pull substituent patterns seem to largely cancel whatever small influence the individual groups exert on the isomerization energetics (entries 11–13). Changing the metal to Fe is disadvantageous by approximately 5 kcal mol<sup>-1</sup> (entry 15), to Os by about 10 kcal mol<sup>-1</sup> (entry 18),<sup>[2h]</sup> mixed metallic systems furnishing intermediate values (entries 14, 16, and 17). As indicated by entries 35–37 for Fe, substituent effects appear to parallel those found for Ru. Modifying the last variable, L, can have more pronounced consequences than that of substituents described above. For Ru, electron acceptors change the Δ*H*<sub>storage</sub> from fairly little (entries 19 and 20) to more noticeable (entries 21–23; cf. PF<sub>3</sub>, 15.2 kcal mol<sup>-1</sup>; entry 23). Interestingly, strong donors (PH<sub>3</sub>, AsH<sub>3</sub>, and NH<sub>3</sub>) reduce this number to the point that for the tetraammonia complex the photoisomer is more stable (entries 24–26). Various donor–acceptor combinations lie in-between (entries 27–30), a trend mimicked for the Fe analogues (entries 31–34). An attempt to rationalize the computed results is made difficult by the delocalized nature of both topologies,<sup>[2j,4]</sup> which obviates the ability to pinpoint the consequences of structural alteration, although it appears that the relative invariance of the heat storing capacity is the result of counteracting trends. Taking the reductionist approach of focusing on the bonds broken (Cp–Cp and M–M') and bonds made (2σCp–M), the effect of electron-withdrawing R groups may be a dominating relatively stabilizing influence on the photoisomer, strengthening the polarized metal–carbon bond and thus diminishing Δ*H*<sub>storage</sub>. Conversely, donating R groups would cause the opposite.<sup>[5]</sup> Similarly, the Cp–M bond might be stabilized by L=donor, destabilized by L=acceptor. The starting Fv complex, with its lower oxidation state metal, would be less subject to polarizing effects.<sup>[6]</sup> Steric effects of L on both parent and photoisomer constitute another variable. Be that as it may, it is clear that increasing significantly the amount of stored energy on photoisomerization will need a more profound restructuring of the framework than those in Table 1.

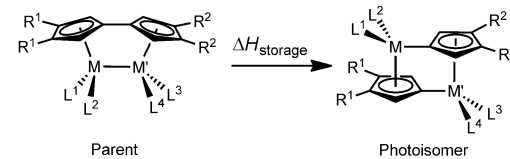
In this vein, it was of interest to probe how the steric encumbrance anticipated for Fv complexes substituted at the α-, or 1,1'(4')-positions would affect the thermodynamics of the photostorage loop. A predictive assessment is not trivial. Thus, while such substitution will clearly strain the parent Fv frame [in **1a** (for numbering see Scheme 1), the respective distances (in silico) of H1 to the juxtaposed C<sub>4br</sub>, C4', and H4' nuclei of the second Cp ring (see Scheme 1 for numbering and the Supporting Information for xyz tables) are 2.95, 2.99, and 2.48 Å],<sup>[2h]</sup> the photoisomer topology may be comparably strained [closest distances of H1 to C<sub>4br</sub>, C1', Ru2, C<sub>CO</sub>, and H1' nuclei of the opposing CpRu(CO)<sub>2</sub> moiety are 3.43, 3.29, 3.53, 3.50, and 2.86 Å]. The energetic cost of minimizing the subvan der Waals separations ensuing on replacement of H1 with another appendage will be determined ultimately by the “floppiness” of the overall structure. A collection of examples addressing this point with Ru derivatives of FvM<sub>2</sub>(CO)<sub>4</sub> is shown in Table 2.

**Table 1.** DFT estimates of  $\Delta H_{\text{storage}}$  by the  $(2,2'-R^1-3,3'-R^2)\text{FvM}_2\text{L}_4$  frame (M = Fe, Ru, Os).



Entry	R	M	L	$\Delta H_{\text{storage}}$ [kcal mol <sup>-1</sup> ]
1 (cf. <b>1a</b> → <b>2a</b> )	R <sup>1,2</sup> = H	M = M' = Ru	L <sup>1-4</sup> = CO	20.8, <sup>[a], [2h]</sup> 20.1 <sup>[b]</sup>
2	R <sup>1,2</sup> = OH	M = M' = Ru	L <sup>1-4</sup> = CO	22.1, <sup>[a]</sup> 21.8 <sup>[b]</sup>
3 (cf. <b>1b</b> → <b>2b</b> )	R <sup>1,2</sup> = tBu	M = M' = Ru	L <sup>1-4</sup> = CO	21.8, <sup>[a]</sup> 21.0 <sup>[b]</sup>
4	R <sup>1,2</sup> = Me	M = M' = Ru	L <sup>1-4</sup> = CO	21.7 <sup>[a]</sup>
5 (cf. <b>8</b> )	R <sup>1,2</sup> = C <sub>6</sub> H <sub>5</sub>	M = M' = Ru	L <sup>1-4</sup> = CO	22.5 <sup>[b]</sup>
6	R <sup>1,2</sup> = Cl	M = M' = Ru	L <sup>1-4</sup> = CO	20.1 <sup>[a]</sup>
7	R <sup>1,2</sup> = CF <sub>3</sub>	M = M' = Ru	L <sup>1-4</sup> = CO	19.4 <sup>[a]</sup>
8	R <sup>1,2</sup> = NO <sub>2</sub>	M = M' = Ru	L <sup>1-4</sup> = CO	18.5, <sup>[a]</sup> 17.6 <sup>[b]</sup>
9 (cf. <b>20</b> → <b>21</b> )	R <sup>1</sup> = benzo (indenyl ligand), one R <sup>2</sup> = tBu, second R <sup>2</sup> = H	M = M' = Ru	L <sup>1-4</sup> = CO	20.0, <sup>[a]</sup> 19.0 <sup>[b]</sup>
10	R <sup>1</sup> = benzo (indenyl ligand), R <sup>2</sup> = H	M = M' = Ru	L <sup>1-4</sup> = CO	19.3 <sup>[a]</sup>
11	R <sup>1</sup> = NMe <sub>2</sub> , R <sup>2</sup> = NO <sub>2</sub>	M = M' = Ru	L <sup>1-4</sup> = CO	22.0 <sup>[a]</sup>
12	R <sup>1</sup> = OH, R <sup>2</sup> = CF <sub>3</sub>	M = M' = Ru	L <sup>1-4</sup> = CO	21.5 <sup>[a]</sup>
13	R <sup>1</sup> = OH, R <sup>2</sup> = NO <sub>2</sub>	M = M' = Ru	L <sup>1-4</sup> = CO	21.5, <sup>[a]</sup> 20.6 <sup>[b]</sup>
14 (cf. <b>27</b> )	R <sup>1,2</sup> = H	M = Ru, M' = Fe	L <sup>1-4</sup> = CO	18.0 <sup>[a]</sup>
15	R <sup>1,2</sup> = H	M = M' = Fe	L <sup>1-4</sup> = CO	15.9, <sup>[a], [2h]</sup> 15.4 <sup>[b]</sup>
16	R <sup>1,2</sup> = H	M = Ru, M' = Os	L <sup>1-4</sup> = CO	12.1 <sup>[a]</sup>
17	R <sup>1,2</sup> = H	M = Fe, M' = Os	L <sup>1-4</sup> = CO	11.0 <sup>[a]</sup>
18 (cf. <b>24</b> → <b>25</b> )	R <sup>1,2</sup> = H	M = M' = Os	L <sup>1-4</sup> = CO	10.2 <sup>[a], [2h]</sup>
19	R <sup>1,2</sup> = H	M = M' = Ru	L <sup>1-4</sup> = CS	20.7 <sup>[a]</sup>
20	R <sup>1,2</sup> = H	M = M' = Ru	L <sup>1-4</sup> = H <sub>2</sub>	20.3 <sup>[a]</sup>
21	R <sup>1,2</sup> = H	M = M' = Ru	L <sup>1-4</sup> = 2,2'-bipy (bidentate)	16.3 <sup>[a]</sup>
22	R <sup>1,2</sup> = H	M = M' = Ru	L <sup>1-4</sup> = P(OH) <sub>3</sub>	17.3 <sup>[a]</sup>
23	R <sup>1,2</sup> = H	M = M' = Ru	L <sup>1-4</sup> = PF <sub>3</sub>	15.2 <sup>[a]</sup>
24	R <sup>1,2</sup> = H	M = M' = Ru	L <sup>1-4</sup> = PH <sub>3</sub>	10.9 <sup>[a]</sup>
25	R <sup>1,2</sup> = H	M = M' = Ru	L <sup>1-4</sup> = AsH <sub>3</sub>	9.3 <sup>[a]</sup>
26	R <sup>1,2</sup> = H	M = M' = Ru	L <sup>1-4</sup> = NH <sub>3</sub>	-1.2, <sup>[a]</sup> -3.5 <sup>[b]</sup>
27	R <sup>1,2</sup> = H	M = M' = Ru	L <sup>1,2</sup> = 2,2'-bipy (bidentate), L <sup>3,4</sup> = CO	18.7 <sup>[b]</sup>
28	R <sup>1,2</sup> = H	M = M' = Ru	L <sup>1,2</sup> = PEt <sub>3</sub> , L <sup>3,4</sup> = CO	18.6 <sup>[b]</sup>
29 (cf. <b>22</b> → <b>23</b> )	R <sup>1,2</sup> = H	M = M' = Ru	L <sup>1</sup> = PEt <sub>3</sub> , L <sup>2</sup> = CO	17.3 <sup>[b]</sup>
30	R <sup>1,2</sup> = H	M = M' = Ru	L <sup>1,2</sup> = PH <sub>3</sub> , L <sup>3,4</sup> = CO	17.2 <sup>[b]</sup>
31	R <sup>1,2</sup> = H	M = M' = Fe	L <sup>1,2</sup> = PEt <sub>3</sub> , L <sup>3,4</sup> = CO	16.5 <sup>[b]</sup>

**Table 1.** (Continued)



Entry	R	M	L	$\Delta H_{\text{storage}}$ [kcal mol <sup>-1</sup> ]
32	R <sup>1,2</sup> = H	M = M' = Fe	L <sup>1,2</sup> = 2,2'-bipy (bidentate), L <sup>3,4</sup> = CO	14.6 <sup>[b]</sup>
33	R <sup>1,2</sup> = H	M = M' = Fe	L <sup>1,2</sup> = PH <sub>3</sub> , L <sup>3,4</sup> = CO	14.0 <sup>[b]</sup>
34	R <sup>1,2</sup> = H	M = M' = Fe	L <sup>1</sup> = PEt <sub>3</sub> , L <sup>2</sup> = CO	12.4 <sup>[b]</sup>
35	R <sup>1,2</sup> = OH	M = M' = Fe	L <sup>1-4</sup> = CO	16.0 <sup>[b]</sup>
36	R <sup>1</sup> = OH, R <sup>2</sup> = NO <sub>2</sub>	M = M' = Fe	L <sup>1-4</sup> = CO	15.8 <sup>[b]</sup>
37	R <sup>1,2</sup> = NO <sub>2</sub>	M = M' = Fe	L <sup>1-4</sup> = CO	13.9 <sup>[b]</sup>

[a] Method: DFT-PBE with plane-wave basis (PBE/PW). PBE = functional of Perdew, Burke, and Ernzerhof.<sup>[3]</sup> [b] Method: BP86/LanL2dz&631 + g(d,p).

Specifically, starting with singly 1-substituted systems (entries 1–5), a cursory inspection of the  $\Delta H_{\text{storage}}$  values ( $\sim 20$  kcal mol<sup>-1</sup>) appears to indicate a negligible effect of the added substituent. That this conclusion is overly simple is revealed when one compares the heats of formation of the individual molecules with those of their corresponding unstrained  $\beta$ -isomers (entries 6–10), tabulated as the hypothetical  $\Delta H_{\text{isomerization}}$  of the  $\alpha$ - to the  $\beta$ -form in the last two columns of Table 2. It can be seen that both the parent and its photoisomer are activated to a similar extent by  $\alpha$ -substitution, leading to a largely attenuated effect on  $\Delta H_{\text{storage}}$ . Not surprisingly, the steric burden of R, as reflected in its corresponding  $\Delta H_{\text{isomerization}\alpha \rightarrow \beta}$ , does not correlate with axial cyclohexane conformational energies, since the structural impediment is very different.<sup>[8]</sup> A slight outlier in the series of entries 1–5 is the last entry, featuring the NMe<sub>2</sub> substituent, which not only raises the energies of both the parent and its photoisomer relative to their  $\beta$  counterparts by relatively large amounts (6.5 and 10.0 kcal mol<sup>-1</sup>, respectively), but does so to a larger extent in the latter. For the former (and relative to the  $\beta$ -isomer), the respective distances of N to the juxtaposed C4b (3.16 Å), C4' (3.14 Å), and H4' nuclei (2.53 Å) of the opposing Cp ring are kept at van der Waals separations<sup>[9]</sup> by increasing the Fv bend (Cp-Cp interplanar angle) from 23.9° to 29.2° and altering the corresponding twist (Cp1<sub>centroid</sub>-Ru1-Ru2-Cp2<sub>centroid</sub>) from 5.2° to -4.2° (moving the NMe<sub>2</sub> unit away from the Fv core). In addition, the nitrogen is more extensively pyramidalized (the N lies above the C substituent plane by 0.35 Å versus 0.26 Å) and the NMe<sub>2</sub> substituent rotated out of co-planarity with the attached Cp by 56.6° (versus 25.8°) in an attempt to minimize the steric impingement of the Me entity. In the corresponding photoisomer, moving the substituent from the  $\beta$  to  $\alpha$  position induces a twist (Cp1<sub>centroid</sub>-Ru1-Cp2<sub>centroid</sub>-Ru2) change from 2.8° to -1.5°. More prominently, the NMe<sub>2</sub> substituent retains the extensive co-planarity with

**Table 2.** DFT estimates of  $\Delta H_{\text{storage}}$  by the FvRu<sub>2</sub>(CO)<sub>4</sub> frame bearing substituents at the  $\alpha$ -positions in comparison with their  $\beta$ -isomers.<sup>[a]</sup>

Entry	Fv substitution pattern	$\Delta H_{\text{storage}}$ [kcal mol <sup>-1</sup> ]	$\Delta H_{\text{isomerization}\alpha\rightarrow\beta}$ [kcal mol <sup>-1</sup> ] parent photoisomer	
1	R = NO <sub>2</sub>	18.6	2.5	1.5
2	R = CO <sub>2</sub> CH <sub>3</sub>	20.4	1.5	1.9
3 (cf. 16→18)	R = C <sub>5</sub> H <sub>4</sub> Re(CO) <sub>3</sub>	20.5	3.3	3.5
4 (cf. 12→14)	R = 2-cyclopentene-1-yl	21.7	2.8	4.6
5	R = NMe <sub>2</sub>	23.8	6.5	10.0
6	R = NO <sub>2</sub>	19.6		
7	R = CO <sub>2</sub> CH <sub>3</sub>	20.0		
8 (cf. 17→19)	R = C <sub>5</sub> H <sub>4</sub> Re(CO) <sub>3</sub>	20.3		
9 (cf. 13→15)	R = 2-cyclopentene-1-yl	19.9		
10	R = NMe <sub>2</sub>	20.3		
11	R = NO <sub>2</sub>	16.8	5.6	3.3
12 (cf. 10→11)	R = CO <sub>2</sub> CH <sub>3</sub>	19.6	4.3	4.1
13	R = NMe <sub>2</sub>	26.4	12.7	18.7
14	R = NO <sub>2</sub>	8.6	12.8	2.3
15	R = CO <sub>2</sub> CH <sub>3</sub>	11.8	11.6	3.6
16	R = NMe <sub>2</sub>	18.0	20.9	18.5
17	R = NO <sub>2</sub>	19.1		
18	R = CO <sub>2</sub> CH <sub>3</sub>	19.8		
19	R = NMe <sub>2</sub>	20.4		
20 (cf. 4 and Table 1, entry 3)	R = <i>t</i> Bu	24.6	-5.9 (14.1) <sup>[b]</sup>	-2.3 (17.7) <sup>[b]</sup>
21 (cf. 9)	R = C <sub>6</sub> H <sub>5</sub>	23.8	1.6	2.9

[a] Method: BP86/LanI2dz&631 + g(d,p). [b] Corrected for the estimated strain in 2,2',3,3'-tetra-*tert*-butylfulvalene, approximately 20 kcal mol<sup>-1</sup>.<sup>[7]</sup>

the attached Cp of the  $\beta$  isomer (23.7° → 24.5°), placing one of the Me groups in close proximity to the facing Ru(CO) segment, increasing the connecting bond lengths and angles (e.g., C1-C4a-Ru2 123.8 → 135.8; C4a-Ru2-C(O) 93.9 → 102.5).

Introduction of a second  $\alpha$  substituent at C1' (Table 2, entries 11–13) leads to  $\Delta H_{\text{storage}}$  numbers that reflect a roughly additive (cf.  $\Delta H_{\text{isomerization}\alpha\rightarrow\beta}$  values of entries 1, 2, and 5) effect of strain (relative to the corresponding  $\beta,\beta'$ -isomers, entries 17–

19) on each member of the photostorage cycle. Thus, for the 1,1'-bis(dimethylamino) derivative (entry 13), the steric activation of the parent, 12.7 kcal mol<sup>-1</sup>, is close to 2 × 6.5 kcal mol<sup>-1</sup> (from entry 5), that of the photoisomer, 18.7 kcal mol<sup>-1</sup>, close to 2 × 10.0. Such additivity for the photoisomeric series was somewhat unexpected, as one might have thought that the transannular proximity of the substituents (at C1 and C1') would add a repulsive increment. However, such is not the case. The "record" size of the computed  $\Delta H_{\text{storage}}$  of entry 13 indicates a possible avenue of further exploration.

With the preceding discussion in mind, the results of 1,4'-disubstitution in entries 14–16 are not surprising.  $\Delta H_{\text{storage}}$  diminishes, because the parent structure is more activated than that of the photoisomer due to the added 1,4'-interaction. Comparison of the  $\Delta H_{\text{isomerization}\alpha\rightarrow\beta}$  for the parent molecules in entries 14–16 with those of entries 11–13 shows that for the substituents investigated this extra destabilization is about 7–8 kcal mol<sup>-1</sup>. A similar comparison of the data for the photoisomer (entries 11–13 versus 14–16), confirms the above conclusion of the absence of transannular in 1,1'-substituted derivatives: they are essentially the same.

The 1,1',3,3'-tetra-*tert*-butylfulvalene system of entry 20 (vide infra, complex 4) exhibits again, and now considerable, strain activation of both parent and photoisomer relative to the 2,2',3,3'-analogue (after correcting for the "ortho"-di-*tert*-butyl contribution in the latter). In the parent structure, it is manifested in large Fv bend (Cp1<sub>plane</sub>-Cp2<sub>plane</sub> 37.4°) and twist angles (Cp1<sub>centroid</sub>-Ru1-Ru2-Cp2<sub>centroid</sub> 23.8°), in the photoisomer in long bonds and angles along the C1-C4a-Ru2-C(O) trajectory. While both  $\Delta H_{\text{isomerization}\alpha\rightarrow\beta}$  values are sizeable, their difference, 3.6 kcal mol<sup>-1</sup> is modest, not unlike the case of NMe<sub>2</sub> ( $\Delta H_{\text{isomerization}\alpha\rightarrow\beta}$  = 3.5 kcal mol<sup>-1</sup>, entry 5).

The findings summarized in Table 2 point to the need for the design of  $\alpha$  substituents that impact the steric encumbrance of photoisomer more than that of the parent by exploiting the distinctly different geometric origins of this interaction. Such might be achieved by rigid fusion of appropriately adorned bicyclic rings, currently under scrutiny.

#### (Tetra-*tert*-butylfulvalene)tetracarbonyldiruthenium complexes 1b and 4

An essential design component of an eventual device<sup>[2e]</sup> was the requirement of high concentrations of the photostorage molecule in solution, since its conversion in the solid (1a and 1b) or neat (thin film of 1c,d) was unsuccessful. Qualitatively, the parent 1a is relatively poorly soluble in CHCl<sub>3</sub>, acetone, C<sub>6</sub>H<sub>6</sub>, and toluene. Quantitatively, it dissolves best in THF to the extent of 21.6 mg mL<sup>-1</sup>. While this value was good enough for the exploration of its chemistry,<sup>[2j]</sup> it was deemed insufficient for the clear demonstration of a temperature rise in the thermal release part of a device. Attention therefore turned to the much more soluble tetra-*tert*-butyl derivative 1b, originally prepared solely for the purposes of demonstrating the synthetic and spectroscopic utility of the ligand in organometallic transformations.<sup>[2j]</sup> Indeed, a solvent screen (see the Supporting Information) revealed again THF as the optimal medium, but



now at 276 mg mL<sup>-1</sup>. Encouraged by this finding, a more complete study of the system **1b** ⇌ **2b** was undertaken (see also Table 1, entry 3, and ref. [2f]), encompassing structural, kinetic, and thermodynamic studies.

The structure of **1b** is shown in Figure 1 (Table 5). Comparison of its bond lengths and angles with those of **1a** reveal a scaffold that is remarkably unperturbed by the *tert*-butyl substitution, with the exception of the expectedly elongated C2–C3 and C8–C9 linkages. The geometry of the molecule is very similar to that of the corresponding Fe and Os analogues,<sup>[2i]</sup> taking into account variations induced by the nature of the respective metal (Figure 1, caption).

As reported, **1b** converts to **2b** quantitatively by irradiation with 350 nm light in a Pyrex vessel.<sup>[2i]</sup> The structure of **2b** is depicted in Figure 2 (Table 5) and is, again, a close replica of the parent system **2a**, but for the stretched *t*BuC–C*t*Bu bonds.

Kinetic experiments for the thermal reversion **2b** → **1b** were executed in toluene, exhibiting clean first-order behavior over a temperature range of 60–100 °C, with  $\Delta H^\ddagger = 25.0 (\pm 0.96)$  kcal mol<sup>-1</sup> and  $\Delta S^\ddagger = -4.5 (\pm 2.7)$  e.u. Switching to diglyme as the solvent produced  $\Delta H^\ddagger = 24.1 (\pm 1.1)$  kcal mol<sup>-1</sup>,  $\Delta S^\ddagger = -6.6 (\pm 3.6)$  e.u. The corresponding numbers for **2a** → **1a** (diglyme) are  $\Delta H^\ddagger = 29.9 (\pm 2)$  kcal mol<sup>-1</sup>,  $\Delta S^\ddagger = 17 (\pm 2)$  e.u.,<sup>[2j]</sup>

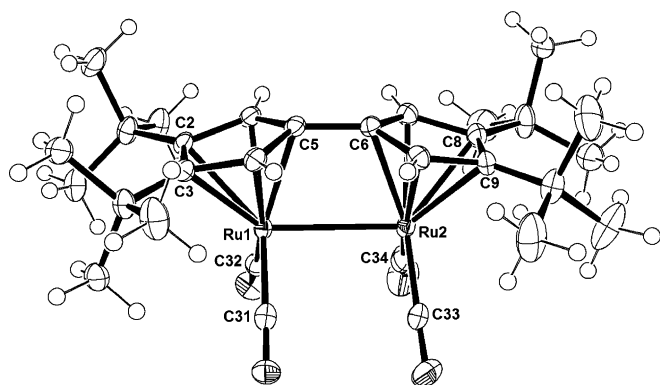


**Figure 1.** ORTEP rendition of **1b** with thermal ellipsoids at 50% probability. There is disorder in the *tert*-butyl group at C8; only one rotamer is shown. Selected bond lengths [Å] and angles [°] in comparison to those of experimentally determined **1a** (in curly brackets):<sup>[2j]</sup> Ru1–Ru2 2.8199(4) {2.821}, Cp1<sub>centroid</sub>–Ru1 1.890 {1.895}, Ru1–C5 2.203(3) {2.223}, C5–C6 1.462(4) {1.457}, Ru1–C31 1.865(3) {1.860}, Ru1–C32 1.862(3) {1.866}, Cp2<sub>centroid</sub>–Ru2 1.897 {1.896}, Ru2–C6 2.238(3) {2.241}, Ru2–C33 1.867(3) {1.870}, Ru2–C34 1.864(4) {1.886}, C2–C3 1.447(4) {1.398}, C8–C9 1.450(4) {1.412}; Ru2–Ru1–C5 73.93(7) {72.44}, Ru1–Ru2–C6 70.45(7) {71.93}, Ru1–C5–C6 105.77(18) {107.92}, C5–C6–Ru2 109.84(18) {107.58}, Ru1–C5–C6–Ru2 1.1(2) {3.57}, C31–Ru1–Ru2–C33 4.34(14) {3.39}, Cp1<sub>centroid</sub>–Ru1–Ru2–Cp2<sub>centroid</sub> 0.39 {4.34}, Cp1<sub>plane</sub>–Cp2<sub>plane</sub> (fulvalene bend) 27.3 {28.5}. Selected comparative values of the Fe (**28**; vide infra, Scheme 10) and Os (**24**; vide infra, Scheme 9) analogues (numbering as in the diagram above):<sup>[2i]</sup> Fe: Fe1–Fe2 2.773(1), Cp1<sub>centroid</sub>–Fe1 1.715, Fe1–C5 2.078(5), C5–C6–Fe2 105.3(3), Fe1–C31 1.750(5), Fe1–C32 1.752(5), Cp2<sub>centroid</sub>–Fe2 1.714, Fe2–C6 2.056(4), Fe2–C33 1.751(5), Fe2–C34 1.757(5), C2–C3 1.459(6), C8–C9 1.457(6); Fe2–Fe1–C5 68.9(1), Fe1–Fe2–C6 73.4(1), Fe1–C5–C6 112.4(3), C5–C6–Fe2 105.3(3), Cp1<sub>centroid</sub>–Fe1–Fe2–Cp2<sub>centroid</sub> 0.5, Cp1<sub>plane</sub>–Cp2<sub>plane</sub> (fulvalene bend) 30.0. Os: Os1–Os2 2.8316(8), Cp1<sub>centroid</sub>–Os1 1.906, Os1–C5 2.23(1), C5–C6 1.44(2), Os1–C31 1.86(2), Os1–C32 1.86(2), Cp2<sub>centroid</sub>–Os2 1.905, Os2–C6 2.25(1), Os2–C33 1.84(2), Os2–C34 1.88(3), C2–C3 1.43(2), C8–C9 1.46(2); Os2–Os1–C5 73.3(3), Os1–Os2–C6 70.6(4), Os1–C5–C6 106.3(9), C5–C6–Os2 109.8(9), Cp1<sub>centroid</sub>–Os1–Os2–Cp2<sub>centroid</sub> 0.1, Cp1<sub>plane</sub>–Cp2<sub>plane</sub> (fulvalene bend) 28.1.

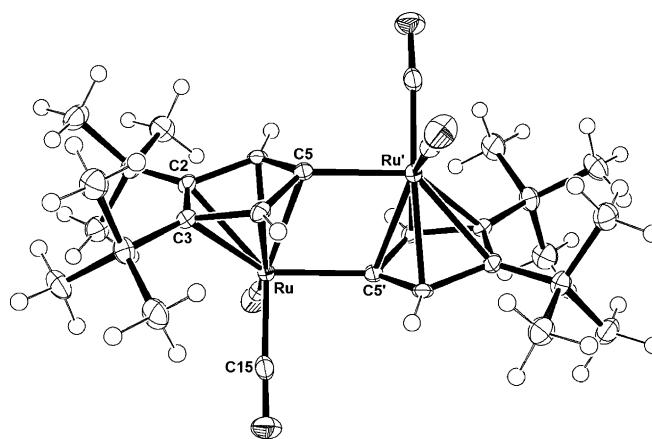
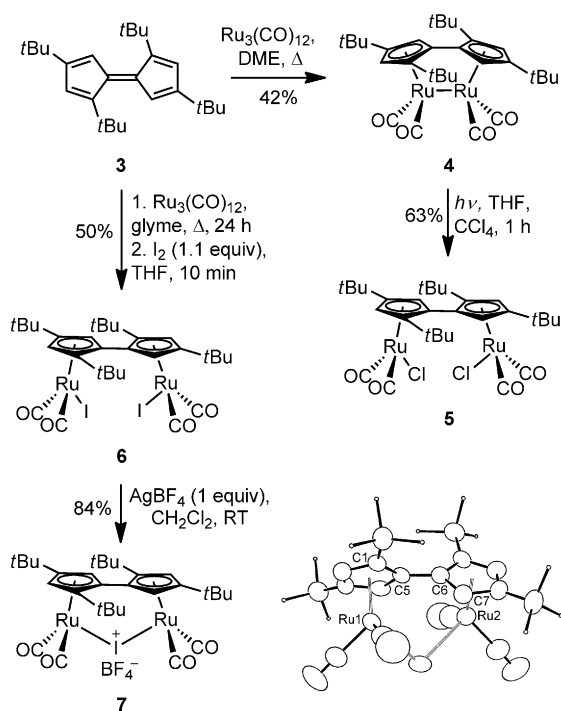


**Figure 2.** ORTEP rendition of **2b** with thermal ellipsoids at 50% probability. The structure has an inversion center. Selected bond lengths [Å] and angles [°] in comparison to those of experimentally determined **2a** (average of two molecules in the unit cell, in curly brackets):<sup>[11h,i]</sup> Ru–Ru' 3.472(1) {3.465}, Cp<sub>centroid</sub>–Ru 1.893 {1.886}, Ru–C5 2.268(3) {2.261}, Ru–C5' 2.075(3) {2.086}, Ru–C15 1.874(3) {1.869}, C2–C3 1.443(4) {1.395}; C5–Ru–C5' 73.89(11) {74.36}, Ru–C5–Ru' 106.11(11), {105.65}, Ru–C5–Ru'–C5' 0 {0}, Cp<sub>centroid</sub>–C5–Ru' 162.74 {162.1}.

for **2c,d** → **1c,d** (toluene)  $\Delta H^\ddagger = 24.0 (\pm 2.0)$  kcal mol<sup>-1</sup>,  $\Delta S^\ddagger = -2.6 (5.6)$  e.u. Finally, the  $\Delta H_{\text{storage}}$  in **2b** was determined by DSC (average of four runs) as 21.1(±2.9) kcal mol<sup>-1</sup>. Overall, and with the caveat that the differences are small, alkyl substitution appears to lower the enthalpy of activation for reversal and increase the amount of stored energy. The accumulated data seemed to bode well for the deployment of **1b** in a device, until it was discovered that, unexpectedly, isomer **2b** precipitated on irradiation of concentrated solutions of **1b**. A solvent screen of **2b** (see the Supporting Information) showed that, while THF is again optimal, it dissolved only 13 mg mL<sup>-1</sup> of the complex, therefore necessitating the development of **1c,d**, as reported elsewhere.<sup>[2e]</sup>

For comparison, a brief exploration of the isomer **4** was undertaken (Table 2, entry 20), readily constructed by treatment of 1,1',3,3'-tetra-*tert*-butylfulvalene (**3**)<sup>[10]</sup> with Ru<sub>3</sub>(CO)<sub>12</sub> in boiling DME (Scheme 2). This ligand, once complexed, had been reported to be rigid and to bind metals diastereoselectively *syn*, retaining its configuration even in the absence of metal–metal bonds, behavior ascribed to the presence of the bulky substituents at the 1,1'-positions.<sup>[11]</sup> Accordingly, only diastereomer **4** was obtained, its structure confirmed by an X-ray structural determination of the iodonium derivative **7** (vide infra, Scheme 2). Two distinct carbonyl carbon peaks are apparent in the <sup>13</sup>C NMR spectrum of **4**, indicative of slow carbonyl exchange.<sup>[2j]</sup>

Since the mechanism of the photoisomerization involves the breaking the Ru–Ru bond to produce a *syn*-biradical that undergoes rotation to its *anti*-conformer, which, in the case of **4**, would eclipse two *tert*-butyl groups, one might expect the photochemistry of **4** to be complicated. Consistent with this notion, irradiation under conditions which led to the rapid conversion of **1a–d** resulted only in the slow disappearance of starting material, as monitored by <sup>1</sup>H NMR spectroscopy, and the emergence of numerous peaks in the fulvalene region.



**Scheme 2.** Synthesis and some reactions of (1,1',3,3'-tetra-*tert*-butylfulvalene)tetracarbonyldiruthenium (4). An ORTEP rendition (50% probability surface) of the cationic portion of 7 is shown at the bottom right (hydrogen atoms are omitted for clarity). Selected bond lengths [Å] and angles [°]: Ru1–Ru2 4.092(1), Ru1–I 2.707(1), Ru2–I 2.717(1); C1–C5–C6–C7 61.8, Cp1<sub>centroid</sub>–Ru1–Ru2–Cp2<sub>centroid</sub> 56.5, Cp1<sub>plane</sub>–Cp2<sub>plane</sub> 59.2.

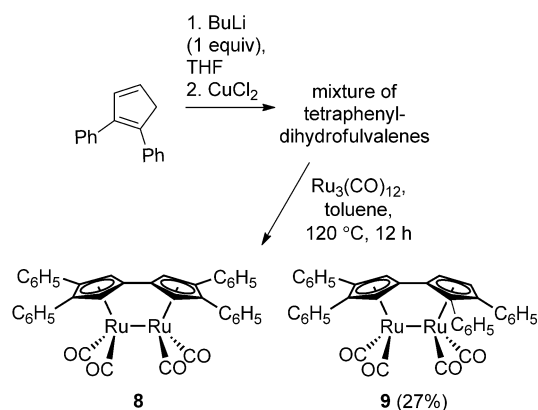
That Ru–Ru bond breaking was occurring was ascertained by executing this experiment with added  $\text{CCl}_4$ , leading to conversion to dichloride 5 (Scheme 2), with spectral data that are in consonance with those of  $\text{FvRu}_2(\text{CO})_4\text{Cl}_2$ , for which the connectivity had been ascertained by X-ray analysis.<sup>[2]</sup> Diiodide 6 was accessed similarly by reaction of 4 with  $\text{I}_2$  and shows spectral data comparable to those of  $\text{FvRu}_2(\text{CO})_4\text{I}_2$  (31, *vide infra*). Finally, treatment of 6 with one equivalent of  $\text{AgBF}_4$  generated iodonium salt 7,<sup>[12]</sup> the X-ray structural determination of which cemented the diastereochemical identity of the series (Scheme 2, Table 5 and the Supporting Information).

### (1,2,2',3'-Tetraphenylfulvalene)tetracarbonyldiruthenium (9)

In view of the above limiting results, attention was turned to phenyl analogues of 1 (cf. Table 1, entry 5), in which the aromatic units should be readily tailorable to meet the challenge of solubility and also provide a platform on which to explore electronic and steric effects of aryl substitution. Thus, 1,2-diphenyl-1,3-cyclopentadiene<sup>[13]</sup> was deprotonated with BuLi and coupled with  $\text{CuCl}_2$  to give an inseparable mixture of tetraphenyldihydrofulvalenes, exhibiting 12 discernible alkenyl hydrogen peaks in the  $^1\text{H}$  NMR spectrum. Treatment of this blend with  $\text{Ru}_3(\text{CO})_{12}$  in toluene at  $120^\circ\text{C}$  gave another mixture from which a yellow fraction was separated by preparative thin layer chromatography, containing mainly unsymmetrical 9, in addition to some of the desired (but not isolated) 8, tentatively

indicated by a singlet at  $\delta = 4.38$  ppm in the  $^1\text{H}$  NMR spectrum (ratio 9/8 = 4:1) (Scheme 3).

Complex 9 (see also Table 2, entry 21) was obtained pure by fractional crystallization (27%), its unsymmetrical nature clearly



**Scheme 3.** Preparation of (1,2,2',3'-tetraphenylfulvalene)tetracarbonyldiruthenium (9).

indicated by the presence of four Fv hydrogen signals in the  $^1\text{H}$  NMR spectrum. The appearance of two broad singlets at 7.67 (1H) and 6.60 ppm (1H), in conjunction with 18  $^{13}\text{C}_{\text{arom}}$  peaks suggests that one of the phenyl groups (presumably that at C1 of the Fv skeleton) exhibits hindered rotation.<sup>[14]</sup> Its encumbered nature (see, e.g., C27–H8 2.638 Å) was ascertained by X-ray crystallography (Figure 3, Table 5).

Attempted photoisomerization of 9 (Rayonet, 350 nm, THF, 3 h), monitored by  $^1\text{H}$  NMR spectroscopy, led to the emergence of 12 new signals in the Fv region and decomposition on prolonged irradiation. It is conceivable that the component stilbene substructures give rise to competing photocyclizations,

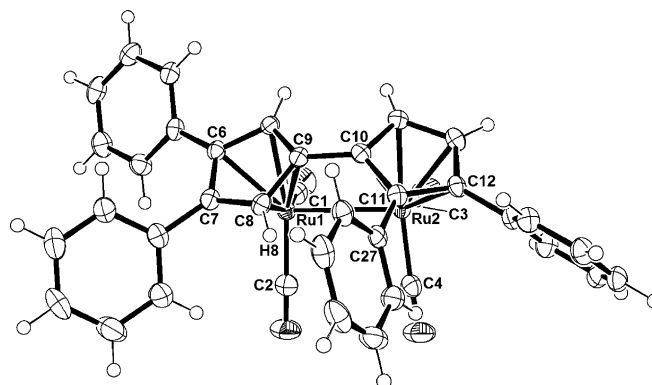


**Figure 3.** ORTEP rendition of 9 with thermal ellipsoids at 50% probability. Selected bond lengths [Å] and angles [°]: Ru1–Ru2 2.8110(4), Cp1<sub>centroid</sub>–Ru1 1.904, Ru1–C9 2.249(3), C9–C10 1.455(4), Ru1–C1 1.863(3), Ru1–C2 1.874(3), Cp2<sub>centroid</sub>–Ru2 1.899, Ru2–C10 2.241(3), Ru2–C3 1.857(3), Ru2–C4 1.879(3), C6–C7 1.438(4), C11–C12 1.442(4), C27–H8 2.638; Ru2–Ru1–C9 71.93(7), Ru1–Ru2–C10 72.85(7), Ru1–C9–C10 108.13(19), C9–C10–Ru2 106.95(18), Ru1–C9–C10–Ru2 –3.64, C2–Ru1–Ru2–C4 –6.24, Cp1<sub>centroid</sub>–Ru1–Ru2–Cp2<sub>centroid</sub> –5.07, Cp1<sub>centroid</sub>–C9–C10–Cp2<sub>centroid</sub> –4.49, C8–C9–C10–C11 –4.92, Cp1<sub>plane</sub>–Cp2<sub>plane</sub> (fulvalene bend) 29.3.

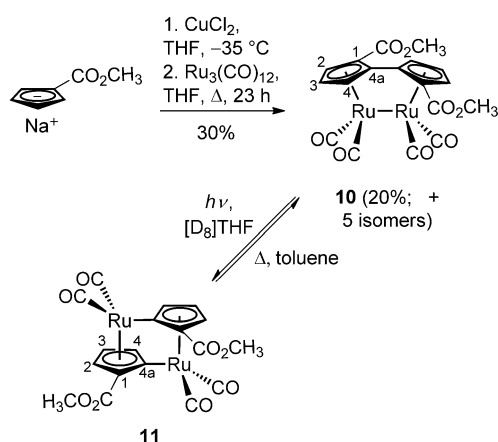
complicating the course of this transformation.<sup>[15]</sup> In support of this possibility, a diagnostic, broad doublet at  $\delta=8.76$  ppm ( $J=8.4$  Hz) infers the formation of a phenanthrene section.

The above failure to effect regioselective oxidative coupling of the 1,2-diphenylcyclopentadienyl anion to generate eventually **8** highlights an inherent limitation of this route to  $\beta$ -substituted fulvalenes,<sup>[2i,4b,16]</sup> which needs bulky substituents to succeed. Phenyl appears deficient in this respect, a problem that may be solved by the introduction of *ortho* groups in the future.

#### (Dimethyl fulvalene-1,1'-dicarboxylate)tetracarbonyldiruthenium (**10**) and isomers

An attempt was made to gain access to water-soluble complexes by introducing the carboxy function, the ultimate aim being the execution of the photostorage cycle in water as a "green" solvent. Such a system also presented an opportunity to test experimentally the repercussions of electron-withdrawing substituents on the photodynamics and, in anticipation of the formation of isomers in the coupling step engendering the fulvalene scaffold, enable a comparison of their relative efficiency in photoisomerizations. Accordingly, methyl sodium cyclopentadienyl anion carboxylate was coupled with  $\text{CuCl}_2$  to the corresponding dihydrofulvalene dicarboxylate giving an extensive mixture of compounds.  $^1\text{H}$  NMR analysis of the dianion ( $\text{BuLi}$ ) showed the predominant presence of the 1,1'-linked species (see the Supporting Information). Treatment of the dihydrofulvalene solution with  $\text{Ru}_3(\text{CO})_{12}$  in boiling THF, followed by extensive chromatographic work-up furnished all six possible diruthenium complexes in poor yield, from which only the dominant 1,1'-dicarboxylate isomer **10** could be obtained pure by crystallization (Scheme 4 and the Supporting Information).

Nevertheless, structural assignments of all isomers could be made by an in-depth NMR analysis, using heteronuclear decoupling, NOE difference,<sup>[17]</sup> homonuclear COSY, and DEPT proce-



**Scheme 4.** Preparation of (dimethyl fulvalene-1,1'-dicarboxylate)tetracarbonyldiruthenium (**10**) and its isomers, and photoisomerization of **10** to **11**. The numbering scheme pertains to the NMR assignments in the Experimental Section.

dures, aided by considerations of symmetry and the observation of deshielding by the carboxy group of its neighboring ring hydrogen atoms and, when located  $\alpha$  (i.e., at C1) of the proximal hydrogen of the opposite ring (i.e., at C4'; see the Supporting Information). Further cementing these assignments was an X-ray structural determination of **10** (Figure 4, Table 5, and the Supporting Information), which reveals a minimal effect of the ester appendages on the topology (see also Table 2, entry 12), boding well for the use of these systems as light energy storage substrates (albeit contingent on a more efficient synthetic access).

A series of experiments confirm the light-induced reorganization of **10** to **11** (Scheme 4), as well as that of the corresponding other isomers, and its thermal reversal (see the Sup-

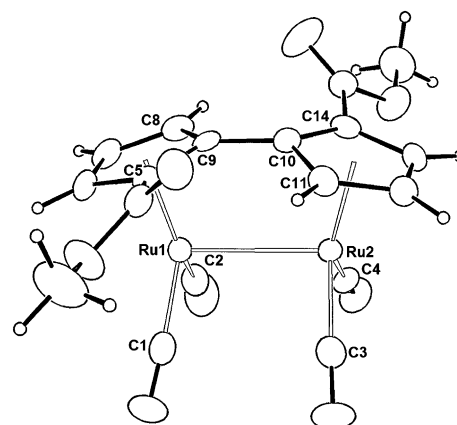


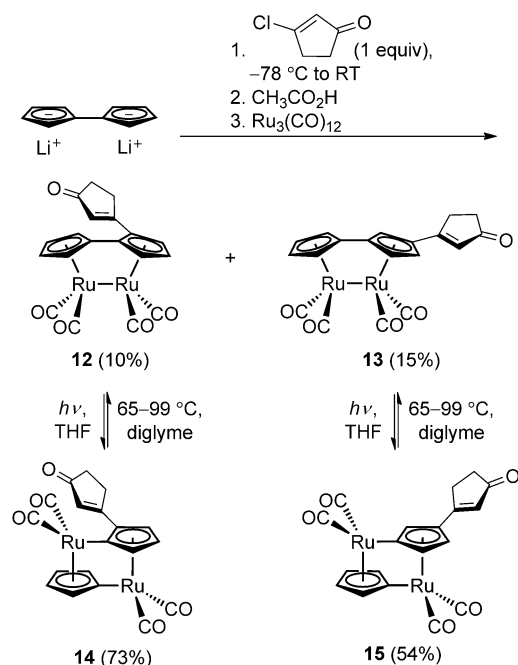
**Figure 4.** ORTEP rendition of **10** (one molecule in the unit cell) with thermal ellipsoids at 50% probability. Selected bond lengths [Å] and angles [°]: Ru1–Ru2 2.807(1), Cp1<sub>centroid</sub>–Ru1 1.894, Ru1–C9 2.227(4), Ru1–C5 2.229(4), C9–C10 1.451(6), Ru1–C1 1.873(5), Ru1–C2 1.866(4), Cp2<sub>centroid</sub>–Ru2 1.900, Ru2–C10 2.243(4), Ru2–C14 2.241(4), Ru2–C3 1.866(5), Ru2–C4 1.857(5); Cp1<sub>centroid</sub>–Ru1–Ru2 105.88, Cp2<sub>centroid</sub>–Ru2–Ru1 105.87, Cp1<sub>centroid</sub>–Ru1–Ru2–Cp2<sub>centroid</sub> –1.52, C5–C9–C10–C11 –1.48, C8–C9–C10–C14 –4.53.

porting Information). Similarly, mixtures of select (dimethyl fulvalenedicarboxylate)tetracarbonyldiruthenium isomers could be hydrolyzed (KOH, EtOH) to the corresponding dicarboxylic acids and shown to undergo thermally reversible photoisomerization (see the Supporting Information). It thus appears that substitution at the  $\alpha$ -positions of the Fv ligand is inconsequential, provided that it is sterically undemanding, and that water-soluble derivatives constitute a viable option in the design of future systems.

#### Selective functional monosubstitution of $\text{FvRu}_2(\text{CO})_4$ : (Tercyclopentadienyl)(tricarbonylrhodium)(tetracarbonyldiruthenium) **16** and **17** and their cyclopentenone precursors **12** and **13**

To further probe the issue of  $\alpha$  versus  $\beta$  substitution, attention turned to complexes **12**, **13**, **16**, and **17** (see also Table 2, entries 8 and 9), which had been disclosed in preliminary form (Scheme 5 and Scheme 6; for the detailed experimental procedures, see the Supporting Information)<sup>[18]</sup> as part of the devel-

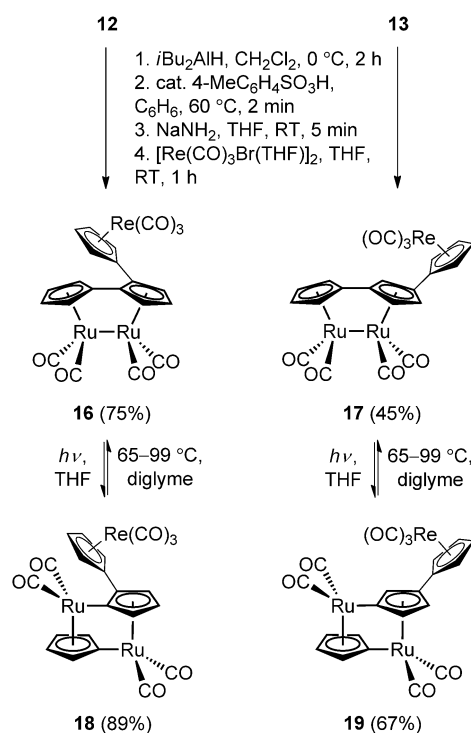
opment of synthetic strategies to “linear” oligocyclopentadienylmetals.<sup>[4a,c]</sup> The regiochemistry of the Fv  $\alpha$ - versus  $\beta$ -substitution in the respective two series was evident from NMR data and confirmed by X-ray structural analyses of **16** and the tungsten analogue of **17**.<sup>[18]</sup>



**Scheme 5.** Synthesis of **12** and **13** and their photoisomerization–thermal reversal relationship with **14** and **15**, respectively.

As anticipated on the basis of the results with **10** and its isomers, the individual cyclopentenone derivatives **12** and **13** converted cleanly (as monitored by <sup>1</sup>H NMR) to the photoisomers **14** and **15**. More informatively, thermal reversal could be quantified through simple first-order kinetics in diglyme, revealing  $\Delta H^\ddagger = 25.4(\pm 0.1)$  kcal mol<sup>-1</sup>,  $\Delta S^\ddagger = 6.9(\pm 0.2)$  e.u. for **14**, and  $\Delta H^\ddagger = 24.9(\pm 1.2)$  kcal mol<sup>-1</sup>,  $\Delta S^\ddagger = 4.9(\pm 3.5)$  e.u. for **15**, very close to each other and the activation parameters for **2b–d** (vide supra). Thus, the electron withdrawing nature of the enone appendages appears have very little influence on the kinetic stability of the photoisomers. Turning to the Re analogues **16** and **17**, irradiation to **18** and **19**, respectively, was uneventful, as was the thermal reverse (Scheme 6):  $\Delta H^\ddagger = 25.1(\pm 0.3)$  kcal mol<sup>-1</sup>,  $\Delta S^\ddagger = 5.1(\pm 0.9)$  e.u. for **18**, and  $\Delta H^\ddagger = 22.3(\pm 3.4)$  kcal mol<sup>-1</sup>,  $\Delta S^\ddagger = -3.6(\pm 9.5)$  e.u. for **19**. In short, all systems behave very much like the parent couple **1a**  $\rightleftharpoons$  **2a**, except for the attenuated enthalpy of activation for the backisomerization of the photoproduct, already noted for the alkyl substituted derivatives **2b–d** (vide supra).

While the photoconversion was not scrutinized in detail, qualitatively all four complexes **12**, **13**, **16**, and **17** isomerize at similar “rates”, implying similar quantum yields. A comparative NMR experiment showed that **16** converted about twice as fast as **17**, a difference too small to be significant. In this connection, one notes that the UV spectra of all examples are

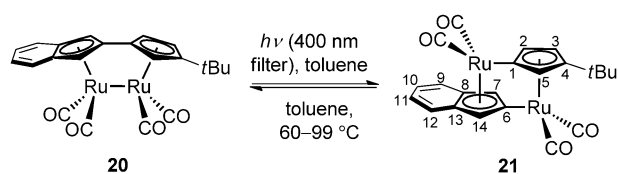


**Scheme 6.** Synthesis of **16** and **17** and their photoisomerization–thermal reversal relationship with **18** and **19**, respectively.

almost identical to that of **1a**, and that, structurally, **16**<sup>[18]</sup> resembles **1a**<sup>[2j,k]</sup> in its essential features.

#### (Benzo[3,4]-3'-*tert*-butylfulvalene)tetracarbonyldiruthenium (**20**)

The known monoindenyl complex **20**<sup>[19]</sup> (Scheme 7; cf. Table 1, entry 9; see the Supporting Information for complete characterization) provided an opportunity to find out whether benzo-fusion would be tolerated by the photostorage system, a desirable feature in the design of examples with chromophores that more effectively overlap with the visible region of the solar spectrum.<sup>[20]</sup> Indeed, relative to the UV spectrum of **1a** [ $\lambda_{\text{max}} = 273, 329, 388$  nm (sh)],<sup>[2k]</sup> that of **20** exhibits significant bathochromic shifts of the pertinent bands [ $\lambda_{\text{max}} = 299, 381, 450$  nm (sh)], qualitatively clearly visible in the change of its color from the yellow of **1a** to deep orange. From a structural perspective, it was also of interest to probe the extent of the operation of any “indenyl effect”.<sup>[21]</sup>



**Scheme 7.** Photothermal cycle **20**  $\rightleftharpoons$  **21**. The numbering scheme pertains to the NMR assignments in the Experimental Section.



Surprisingly, initial attempts to bring about the reorganization of **20** to **21** under standard conditions (Rayonet, using 325 and 375 nm bulbs, or projector lamp, Pyrex vessels) left the starting material untouched. To explain this failure, it was suspected that the added benzofusion had shifted the low energy UV absorptions of **21** into the range of the incoming light, thus thwarting the photobleaching aspect of prior systems by setting up an unfavorable photostationary equilibrium. Support for this notion came from experiments that suggested that more energetic photolysis of **2a** (quartz vessels,  $\lambda_{\text{max}} < 300$  nm) caused rapid rearrangement to **1a** (in this case followed by decarbonylation).<sup>[2]</sup> Gratifyingly, irradiation of **20** through an aqueous NaNO<sub>2</sub> filter (75% w/v; 400 nm cutoff)<sup>[22]</sup> proceeded cleanly to **21** (<sup>1</sup>H NMR). Notably, and in consonance with the preceding thoughts, its highest wavelength  $\lambda_{\text{max}}$  occurs at 357 nm (cf. **2a**  $\lambda_{\text{max}} = 286$  nm).<sup>[22]</sup> This phenomenon may constitute a “catch 22” limitation in the design of future sunlight energy harvesting variants, as expanding the electronic spectral range of the parent to lower energies can shift the spectrum of the photoisomer in parallel, constraining the size of the workable spectral window.

The structural identity of **21** was evident from its spectral data and was confirmed by an X-ray analysis of crystals formed by slow diffusion of pentane into an Et<sub>2</sub>O solution at 10 °C (Figure 5, Table 5). The principal features around the Cp<sub>2</sub>Ru<sub>2</sub> core resemble those of related complexes, for example, **2a** and **2b** (Figure 2), the additional benzene ring exerting mainly a local perturbation. As for **20**, the indenyl effect is negligible (slip distortion is identical to that of **21**,  $\Delta = 0.116$ ), and the Cp<sub>centroid</sub> distance to Ru1 slightly longer than that to Ru2.<sup>[21]</sup> Consequently, the activation parameters for the thermal reversal **21**→**20** are unexceptional,  $\Delta H^\ddagger = 22.6(\pm 1)$  kcal mol<sup>-1</sup>,  $\Delta S^\ddagger = -12.6(\pm 3)$  e.u.

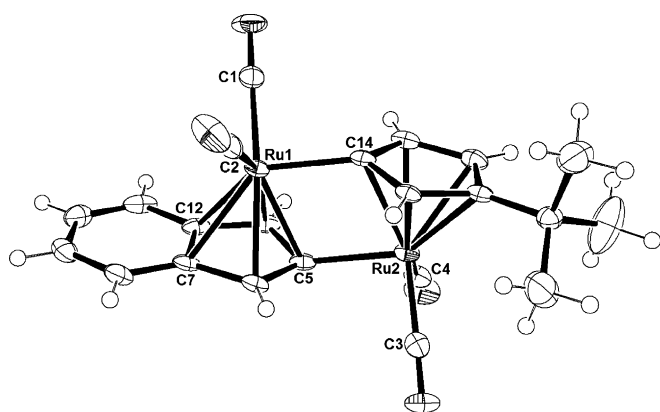
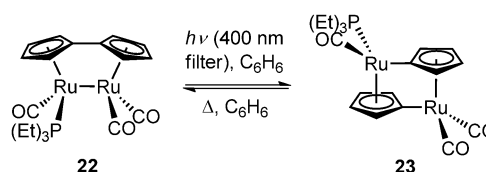


**Figure 5.** ORTEP rendition of **21** with thermal ellipsoids at 50% probability. Selected bond lengths [Å] and angles [°]: Ru1–Ru2 3.454(3), Cp<sub>Indcentroid</sub>–Ru1 1.922, Ru1–C5 2.262(3), Ru1–C14 2.070(3), Ru1–C1 1.888(3), Ru1–C2 1.893(3), C7–C12 1.433(4), Cp<sub>centroid</sub>–Ru2 1.901, Ru2–C14 2.266(3), Ru2–C3 1.880(4), Ru2–C4 1.872(3); C5–Ru1–C14 74.81(11), Ru1–C5–Ru2 105.20(12), Ru1–C14–Ru2 105.53(12), C5–Ru2–C14 74.46(11), Cp<sub>Indcentroid</sub>–C5–Ru2 163.35, Cp<sub>centroid</sub>–C14–Ru1 162.42, Ru1–C14–Ru2–C5 0.23, Cp<sub>Indplane</sub>–Cp<sub>plane</sub> 2.64.

### (Fulvalene)(triethylphosphine)tricarbonyldiruthenium (**22**) revisited

The preceding discovery of the advantageous employment of a 400 nm filter in the conversion of **20** to obviate the detrimental photoactivation of **21** (with a  $\lambda_{\text{max}} > 300$  nm) brought to mind the earlier failure of monotriethylphosphine complex **22** [and its P(Me)<sub>3</sub> relative] to undergo this chemistry (see Table 1, entry 29).<sup>[22]</sup> Similar to the introduction of benzofusion in **20**, substitution of one CO for P(alkyl)<sub>3</sub> causes a substantial redshift of the FvRu<sub>2</sub> chromophore (for **22**,  $\lambda_{\text{max}} = 460$  nm). It was therefore plausible that the seeming inertness of **22** had its origin in the lability of its isomer **23** under the standard photochemical conditions. In agreement with this idea, execution of the photoexperiment with a 400 nm filter gave **23** quantitatively (Scheme 8). As surmised, its electronic spectrum displays absorptions that extend to 425 nm. Unlike **22**, in which a fluxional process [ $\Delta G_{298}^\ddagger = 12.0(\pm 1)$  kcal mol<sup>-1</sup>] involving pairwise bridging carbonyls precipitates intrametallic phosphine site exchange (i.e., racemization), thus giving rise to only four <sup>1</sup>H and ten <sup>13</sup>C NMR signals,<sup>[2]</sup> **23** maintains its asymmetric nature, as expected. Therefore, there are now eight Fv hydrogen absorptions, and the diastereotopic phosphine methylenes give rise to two signals. Similarly, the <sup>13</sup>C NMR spectrum reveals ten peaks for the Fv frame and three for the carbonyls.



**Scheme 8.** Photothermal cycle **22**⇌**23**.

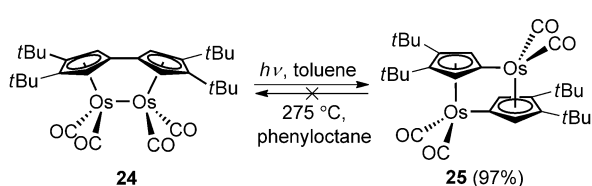
Heating **23** caused clean reversal. While this process was not quantified by kinetic measurements, its speed appears to be comparable to that of the other systems. A qualitative appraisal of relative stability was made by heating an equimolar NMR sample of **2a** and **23** at 75 °C for 10 min, showing a slightly faster appearance of **1a** (21%) compared to **22** (5.7%).

In short, it appears that the FvRu<sub>2</sub> photothermal system can be tailored by substitution of CO with other ligands without detrimental effects on its efficiency, provided that the frequency of the impinging light is regulated appropriately.

### Some comparisons of FvM<sub>2</sub>(CO)<sub>4</sub> (M = Fe, Ru, Os) and synthesis of the mixed metal (fulvalene)tetracarbonyliron-ruthenium (**27**)

It was of fundamental interest to compare the efficacy of the FvRu<sub>2</sub> system to those incorporating the other two metals in the triad, Fe (Table 1, entries 14, 15, 17, and 31–37) and Os (Table 1, entries 16–18). In addition, from a practical device perspective, moving from the expensive and toxic Ru to the cheap and environmentally benign Fe constituted a desirable goal. We have disclosed some experiments along these lines,

which will be summarized briefly in order to place additional results into the proper perspective. Seminal DFT computations on the respective parent complexes revealed that not only are the  $\Delta H_{\text{storage}}$  values diminished for Fe (15.9 kcal mol<sup>-1</sup>) and Os (10.2 kcal mol<sup>-1</sup>) relative to Ru (20.8 kcal mol<sup>-1</sup>), but that the barrier for reversal is much lower for the former (17.3 kcal mol<sup>-1</sup>), much higher for the latter (> 42 kcal mol<sup>-1</sup>).<sup>[2h]</sup> Unsuccessful attempts at the photoisomerization of the Fe analogues of **1 a–d** (various light sources, filters, and temperatures) were blamed on this kinetic lability of the product, until picosecond time-resolved IR experiments uncovered that the system does not even undergo sufficiently fast intersystem crossing from the excited singlet to its triplet relative, necessary for photoconversion.<sup>[2b]</sup> This problem needs to be solved, before tackling the kinetic stability of the photostorage product. Turning to Os, the only derivative that has been accessible (so far) is the structurally characterized tetra-*tert*-butyl Fv complex **24** [for a comparison of selected bond lengths and angles with those in the Fe and Ru (**1 b**), see Figure 1 caption].<sup>[2i]</sup> Cursory examination of its photochemistry had shown that it underwent photoisomerization to **25**, which was stable under conditions in which **2 b** reverted to **1 b**. This matter was reinvestigated, improving yields (see the Supporting Information), particularly that of **25** (quantitative; Scheme 9).



Scheme 9. Photoisomerization of **24** to **25**.

The results of a crystal structure determination of **25** are presented in Figure 6 (Table 5) and can be compared to those of its Ru analogue **2 b** (Figure 2), the minor differences readily attributed to the change in the metal.

As presaged by computation,<sup>[2h]</sup> **25** proved to be inordinately thermally stable and was recovered unchanged from toluene at 120 °C, 1,2-dichlorobenzene at 200 °C, and, finally, 1-phenyloctane at 275 °C (all in sealed tubes), the last conditions causing gradual decomposition after several hours. Similarly, 1% AgNO<sub>3</sub>–SiO<sub>2</sub>, a system that effectively catalyzes the reorganization of **2** to **1** (vide infra), failed to do so for **25**.

In view of the preceding findings, we were curious about the behavior of a mixed metal FvFeRu analogue, in the hope that the Ru atom might facilitate intersystem crossing and also change favorably the kinetic picture of the thermal reverse trajectory. From a practical perspective, if successful, a device would be cheaper and environmentally more tolerable than one based on FvRu<sub>2</sub>, while still endowed with a substantial  $\Delta H_{\text{storage}}$  capability (~18 kcal mol<sup>-1</sup>; Table 1, entry 14). A contemplation of synthetic routes to such a system suggested recourse to strategies for the construction of heterodinuclear Fv complexes, developed earlier by us.<sup>[4a]</sup> However, because they

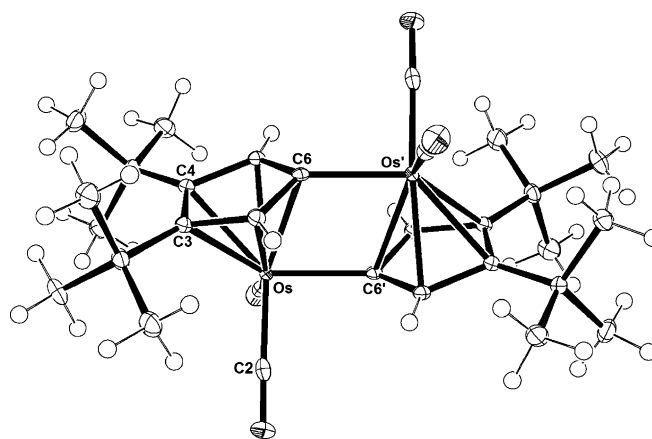
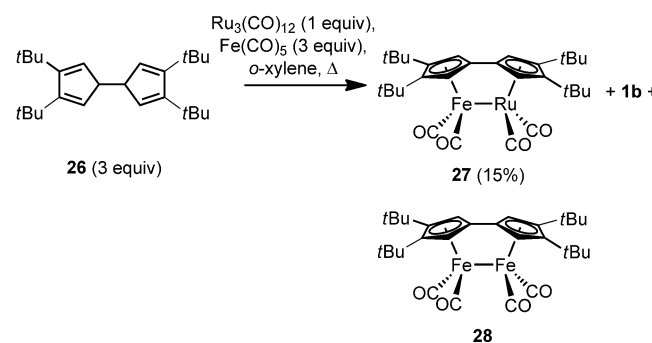


Figure 6. ORTEP rendition of **25** with thermal ellipsoids at 50% probability. The structure has an inversion center. Selected bond lengths [Å] and angles [°]: Os–Os' 3.506(1), Cp<sub>centroid</sub>–Os 1.907, Os–C6 2.293(2), Os–C6' 2.088(2), Os–C2 1.876(3), C3–C4 1.454(4); C6–Os–C6' 73.80(10), Os–C6–Os 106.20(10), Os–C6–Os'–C6' 0, Cp<sub>centroid</sub>–C6–Os' 162.44.

involved several steps, and for the purposes of accessing a test system rapidly, instead the conditions that led to the homodinuclear derivatives of Fe<sup>[2b,i]</sup> and Ru<sup>[2i]</sup> were modified simply by treating **26** with Ru<sub>3</sub>(CO)<sub>12</sub> and Fe(CO)<sub>5</sub> (ratio 3:1:3) in boiling *o*-xylene to generate the tetra-*tert*-butyl heterobimetallic complex **27**, admixed with **28** and **1 b** in the ratio 1:1:1.6 (Scheme 10). This mixture proved to be inseparable by standard techniques, and pure **27** was eventually sequestered by selective destruction of the most sensitive component **28** in the mixture (decomposition in CH<sub>2</sub>Cl<sub>2</sub>) and selective photoconversion of **1 b** to **2 b**, followed by chromatography. The apparent photoinertness of **27** in the mixture was confirmed on pure material (various light sources, filters, and temperatures). It is possible that the lack of efficient intersystem crossing from the excited singlet observed for **28** (and congeners) is the origin of this failure, but this is speculative.

The availability of crystals of **27** suitable for X-ray diffraction provided the opportunity for a structural determination of a unique<sup>[4,23]</sup> Fv complex containing an Fe–Ru bond (Figure 7, Table 5), and to compare its features with those of the homodinuclear relatives **28** (Figure 1 caption) and **1 b** (Figure 1). Interestingly, along the series **28**, **27**, **1 b** all core bond distances in



Scheme 10. Synthesis of heterobimetallic complex **27**.

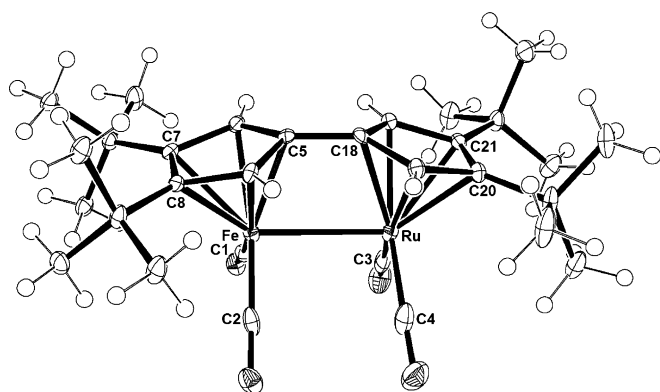


**Figure 7.** ORTEP rendition of **27** with thermal ellipsoids at 50% probability. Selected bond lengths [Å] and angles [°]: Fe–Ru 2.7664(3), Cp<sub>centroid</sub>–Fe 1.790, Fe–C5 2.118(2), C5–C18 1.454(3), Fe–C1 1.784(2), Fe–C2 1.779(3), Cp<sub>centroid</sub>–Ru 1.847, Ru–C18 2.191(2), Ru–C3 1.810(3), Ru–C4 1.807(3), C7–C8 1.456(3), C20–C21 1.454(3); Ru–Fe–C5 75.01(6), Fe–Ru–C18 69.57(6), Fe–C5–C18 105.29(14), C5–C18–Ru 110.14(14), Fe–C5–C18–Ru –0.10, Cp<sub>centroid</sub>–Fe–Ru–Cp<sub>centroid</sub> –0.25, Cp<sub>plane</sub>–Cp<sub>plane</sub> (fulvalene bend) 29.4.

the FvM<sub>2</sub> core (i.e., M–M<sup>(i)</sup>, Cp<sub>centroid</sub>M/M<sup>(i)</sup>, M/M<sup>(i)</sup>–C<sub>Fvlinkager</sub> and Cp–Cp) increase steadily with the exception of the intermetallic separation, which remains relatively short in **27** (2.766 Å; cf. **28**: 2.773 Å, **1b**: 2.820 Å). This effect is absent in the unlinked Cp<sub>2</sub>MM<sup>(i)</sup>(CO)<sub>4</sub> series, with the caveat that two of the carbonyls adopt the bridging configuration [cf. M–M<sup>(i)</sup> *trans*-Cp<sub>2</sub>Fe<sub>2</sub>(CO)<sub>4</sub> 2.534(2) Å,<sup>[24]</sup> *trans*-Cp<sub>2</sub>FeRu(CO)<sub>4</sub> 2.626(1) Å,<sup>[23]</sup> and *trans*-Cp<sub>2</sub>Ru<sub>2</sub>(CO)<sub>4</sub> 2.7377(5) Å<sup>[25]</sup>].

### (Fulvalene)hexacarbonyldimolybdenum **29** and -tungsten **30**

In the search for additional metals that might mimic the chemistry displayed by FvRu<sub>2</sub>, a brief exploration of the relatively cheap and benign Mo and W analogues FvMo<sub>2</sub>(CO)<sub>6</sub> (**29**)<sup>[26,27]</sup> and FvW<sub>2</sub>(CO)<sub>6</sub> (**30**)<sup>[26,28]</sup> was undertaken (see the Supporting Information), discouraging preliminary results in the literature notwithstanding.<sup>[28,29]</sup> The Cr kin was not considered because of its extreme sensitivity<sup>[30]</sup> and because a DFT appraisal [BP86/LanL2dz&631 + g(d,p)] of the photoisomer showed it to be unstable in silico with respect

to unravelling to the *anti*-biradical by Cp–Cp coupling (–21 kcal mol<sup>–1</sup>). On the other hand, the Mo (**29**; Δ*H*<sub>storage</sub> = 24.1 kcal mol<sup>–1</sup>) and W versions (**30**; Δ*H*<sub>storage</sub> = 13.2 kcal mol<sup>–1</sup>) behaved normally. Unfortunately, and confirming previous attempts, irradiation of these compounds (various light sources, filters, and temperatures) left them untouched for several hours, after which (> 10 h) decomposition became evident. Similarly, P(Et)<sub>3</sub> and P(OMe)<sub>3</sub> derivatives of **30** (see the Supporting Information) decomposed to complex mixtures on irradiation at room temperature.

### Catalysis of the thermal reversal

For the purposes of exerting control over the heat-releasing step in a prototype device<sup>[2e]</sup> and for potential practical applications, it was deemed highly desirable to find catalysts that would allow the thermal reversal to occur rapidly at ambient temperature. In setting up screens for potential candidates, preliminary guidance was provided by some indications that the **2a** → **1a** process was accelerated by added ligands L, spe-

**Table 3.** Screen of select nucleophilic ligands for catalytic reversal of **2a** and **2b**.

Entry <sup>[a]</sup>	Photoisomer [mg]	Catalyst [mg]	Time	Result
1	<b>2a</b> (5)	imidazole (1)	24 h	<b>1a</b> , 100%
2	<b>2a</b> (5)	P(C <sub>6</sub> H <sub>5</sub> ) <sub>3</sub> (3)	24 h	<b>1a</b> , 95%; <b>2a</b> , 5%
3	<b>2a</b> (5)	As(C <sub>6</sub> H <sub>5</sub> ) <sub>3</sub> (3.5)	24 h	<b>1a</b> , 95%; <b>2a</b> , 5%
4	<b>2a</b> (5)	P(OC <sub>6</sub> H <sub>5</sub> ) <sub>3</sub> (3.5)	24 h	<b>1a</b> , 50%; unidentified products 50%
5	<b>2a</b> (0.6)	piperidine (16.7)	6.5 h	<b>1a</b> , 61%; <b>2a</b> , 39%
6	<b>2a</b> (0.6)	2,2,6,6-tetramethylpiperidine (32)	6 h	no conversion, solution turns dark
7	<b>2a</b> (0.7)	aniline (7)	5 h	<b>1a</b> , 68%; <b>2a</b> , 32%
8	<b>2a</b> (0.6)	2,4-dimethylaniline (16)	6 h	<b>1a</b> , 67%; <b>2a</b> , 33%
9	<b>2a</b> (0.8)	3-methoxyaniline (19)	6 h	<b>1a</b> , 63%; <b>2a</b> , 37%
10	<b>2a</b> (0.7)	6-methyl-2-pyridinamine (7)	5 h	<b>1a</b> , 42%; <b>2a</b> , 58%
11	<b>2a</b> (0.7)	3-nitroaniline (7)	6 h	<b>1a</b> , 19%; <b>2a</b> , 81%
12	<b>2a</b> (0.6)	4-bromoaniline (6)	5 h	<b>1a</b> , 25%; <b>2a</b> , 75%
13	<b>2a</b> (0.5)	3-(1-hydroxyethyl)aniline (2.5)	5 h	<b>1a</b> , 23%; <b>2a</b> , 77%
14	<b>2a</b> (0.2)	<i>N,N</i> -dimethylaniline (16)	5 h	no conversion
15	<b>2a</b> (0.9)	benzylamine (32)	5 h	<b>1a</b> , 47%; <b>2a</b> , 53%
16	<b>2a</b> (0.5)	1,4-benzenediamine (5)	5 h	<b>1a</b> , 74%; <b>2a</b> , 26%
17	<b>2a</b> (0.5)	1,8-diaminonaphthalene (2.5)	5 h	<b>1a</b> , 16%; <b>2a</b> , 84%
18	<b>2a</b> (0.5)	1,2-ethanediamine (5)	5 h	decomposition
19	<b>2a</b> (0.5)	(2 <i>S</i> ,4 <i>R</i> )-4-hydroxyproline (5)	5 h	no conversion
20	<b>2a</b> (5)	polyacrylonitrile (25)	12 h	no conversion
21	<b>2a</b> (0.6)	imidazole–SiO <sub>2</sub> <sup>[b]</sup> (7)	26.5 h	no conversion
22	<b>2b</b> (5)	MeCN (solvent)	20 min	<b>1b</b> , 100%
23	<b>2b</b> (5)	DMSO (solvent)	15 min	<b>1b</b> , 100%
24	<b>2b</b> (5)	DMF (solvent)	15 min	<b>1b</b> , 100%
25	<b>2b</b> (5)	Et <sub>2</sub> NH (2)	20 min	decomposition
26	<b>2b</b> (5)	benzylamine (2)	20 min	<b>2b</b> ; 50% decomposition
27	<b>2b</b> (5)	P(C <sub>6</sub> H <sub>5</sub> ) <sub>3</sub> (3)	10 h	decomposition

[a] Experimental: **2** in THF (1.0 mL) was treated with the catalyst candidate at RT and conversions was monitored by thin-layer chromatography and <sup>1</sup>H NMR spectroscopy. [b] 3-(Imidazol-1-yl)propyl-functionalized silica gel from Sigma–Aldrich.

cifically CO [ $k(\text{N}_2) = 2.51 \times 10^{-2} \text{ min}^{-1}$  versus  $k(\text{CO}) = 1.35 \times 10^{-1} \text{ min}^{-1}$  in diglyme], MeCN (20 min, complete conversion), and  $\text{PMe}_3$  (8 equiv, 2 h). A change in mechanism was indicated, featuring initial direct nucleophilic addition to Ru, followed by rearrangement to a zwitterion of the type  $\text{Fv}(\text{Ru}(\text{CO})_2\text{L}^+)(\text{Ru}(\text{CO})_2^-)$ , and regeneration of the Ru–Ru bond by extrusion of L, in the case of  $\text{PMe}_3$  prevented by competitive monodereuthenation.<sup>[2j]</sup> The results depicted in Table 3 corroborate and expand on these findings.

Thus, a number of nucleophiles are quite effective in reconstituting **1** from **2** (entries 1–3, 22–24), some less so (entries 5, 7–16), and some are either inactive (entries 6, 14, 19–21) or cause decomposition (entries 4, 18, 25–27). Steric hindrance appears to be disadvantageous (entries 6, 14, 17, 19), as (possibly) are electron-withdrawing groups (entries 4, 10, 11, 19; in addition, 1,2,4-triazole and tetrazole were inert to **2b**, pyridine caused slow decomposition). The tetra-*tert*-butyl derivative **2b** is clearly also more sensitive than **2a** (entries 25–27). Noteworthy is the efficacy of imidazole (entry 1) and the solvents MeCN (vide supra and entry 22), DMSO (entry 23), and DMF (entry 24; but not  $\text{CS}_2$  and  $\text{MeNO}_2$ ). Unfortunately, all transformations were too slow to be practical (one notes that almost all entries in Table 3 employ excess “catalyst”), apart from their homogeneous nature, which obviates their use in a device. Attempts to use immobilized versions of nitrile (entry 20, in addition to SiliaBond Cyano from SiliCycle Inc) or amines (entry 21, in addition to methyl-functionalized polystyrene bearing imidazole,<sup>[31]</sup> aniline,<sup>[32]</sup> and 1,4-benzenediamine functions<sup>[33]</sup>) failed to elicit any turnover of **2**.

Therefore, while these findings were tantalizing, we opted for another possible catalytic pathway, involving metals as one-electron oxidants or Lewis acids. This choice was inspired by the extensive precedence for these alternatives in one of the most investigated organic variants of  $1 \leftrightarrow 2$ , the norbornadiene–quadricyclane system.<sup>[34]</sup> The results are shown in Table 4.

It appears that both Lewis acids and/or potential one-electron oxidants are active, with mixed results, with the exception of  $\text{AgNO}_3$ , either as such (entry 1, 10) or deposited on silica (entries 8, 9, 11). Other metals are either sluggish (entries 2, 4,

7) or deleterious. Some of the recorded decompositions (vide infra and entries 3, 5, 6) may be ascribed to adventitious acid, as we have noted that HI converts **2a** to  $\text{FvRu}_2(\text{CO})_4\text{I}_2$  (**31**) and  $\text{H}_2$  quantitatively (see the Supporting Information).<sup>[37]</sup> Several other species caused disintegration of **2**, such as  $\text{AgBF}_4$ ,  $\text{Ag}(\text{O}_2\text{CCF}_3)$ ,  $\text{AgCl}$ ,  $\text{AgSO}_4$ , Al-SBA-15,<sup>[38]</sup>  $\text{Fe}(\text{NO}_3)_3$ ,  $\text{Pb}(\text{NO}_3)_3$ ,  $\text{PbO}_2$ ,  $\text{WO}_3$ , and  $\text{ZnCl}_2$ -SBA-15,<sup>[39]</sup> attesting to the capriciousness of the Ru complexes. Many additives left **2** intact, for example, Pd/C, Pt/C,  $\text{MnO}_2$ ,  $\text{SeO}_2$ ,  $\text{Ag}_2\text{O}$ ,  $\text{AgSO}_4$ ,  $\text{AgNO}_3$ - $\text{Al}_2\text{O}_3$ ,  $\text{ZnCl}_2$ - $\text{SiO}_2$ ,<sup>[40]</sup>  $\text{AgI}$ - $\text{SiO}_2$ ,<sup>[41]</sup> 3-aminopropyltriethoxysilane (APTS)-SBA-15,<sup>[42]</sup>  $\text{Ag}$ -APTSal-SBA-15,<sup>[43]</sup>  $\text{Ag}$  or  $\text{Fe}$  or  $\text{Cu}$ -(3-imidazol-1-yl)-propyl- $\text{SiO}_2$ ,<sup>[44]</sup>  $\text{Cu}(\text{NO}_3)_2$ ,  $\text{CuSO}_4$ (ethanediamine)<sub>2</sub>,<sup>[45]</sup>  $\text{MgSO}_4$ -ethanediamine (1:1),  $\text{AgNO}_3$ -ethanediamine (1:1),  $\text{NaNO}_3$ ,  $\text{MgSO}_4$ ,  $\text{H}_3\text{PMO}_{12}\text{O}_{40}$ ,  $\text{V}_2\text{O}_5$ , and the metal–organic frameworks Co or Mn(BDP) (BDP<sup>2-</sup> = 1,4-benzenedipyrazolate),<sup>[46]</sup> and Fe(BTT) (BTT<sup>3-</sup> = 1,3,5-benzenetristetrazolate).<sup>[47]</sup>

A curious scenario unfolded when **2a** in THF was treated with charcoal (coconut charcoal; Fisher Scientific), as the solution turned the yellow color anticipated for the formation of **1a**. However, spectral data negated this interpretation and instead pointed to the quantitative formation of  $\text{FvRu}_2(\text{CO})_4\text{I}_2$  (**31**), an outcome deemed sufficiently far-fetched to warrant X-ray crystallographic confirmation. Such is presented in Figure 8 (Table 5), depicting a topology that is essentially isostructural with that of the corresponding dichloride.<sup>[2j]</sup>

It is possible that entrapped  $\text{O}_2$  in the charcoal caused oxidation<sup>[48]</sup> of **2a** with concomitant rearrangement and trapping by iodide impurities, but this aspect was not investigated further. One notes, however, that activated Charcoal Norit (Sigma–Aldrich) was inert.

The superior performance of  $\text{AgNO}_3$ - $\text{SiO}_2$  in these trials led to the implementation of this catalyst in a first-generation device using the  $\text{FvRu}_2$  system **1c, d**  $\leftrightarrow$  **2c, d**.<sup>[2e]</sup> The limited turnover number (~30) in this application appeared to be caused by decomposition to metallic Ag, as indicated by the grey to black coloration of the support in the heat-releasing chamber. Consequently some studies were initiated aimed at delineating further the catalyst’s behavior, focusing on the **1b**  $\leftrightarrow$  **2b** cycle. One percent  $\text{AgNO}_3$ - $\text{SiO}_2$  was prepared from 99.995% purity salt (VWR-Alfa Aesar) and ultrapure silica (Fisher Scientific-

**Table 4.** Screen of select metal species for catalytic reversal of **2a** and **2b**.

Entry <sup>[a]</sup>	Photoisomer [mg]	Catalyst [mg]	Time	Result
1	<b>2a</b> (5)	$\text{AgNO}_3$ (1.9)	24 h	<b>1a</b> , 100%
2	<b>2a</b> (5)	$\text{Cu}(\text{OTf})_2$ (4)	24 h	<b>1a</b> , 70%; <b>2a</b> , 30%
3	<b>2a</b> (5)	$\text{CuCl}_2$ (1.5)	24 h	$\text{FvRu}_2(\text{CO})_4\text{Cl}_2$ , <sup>[2j]</sup> 20%; <b>2a</b> , 80%
4	<b>2a</b> (5)	$\text{ZnCl}_2$ (1.5)	24 h	<b>1a</b> , 50%; <b>2a</b> , 50%
5	<b>2a</b> (5)	$\text{ZnBr}_2$ (2.5)	24 h	<b>1a</b> , 50%; $\text{FvRu}_2(\text{CO})_4\text{Br}_2$ , <sup>[35]</sup> 50%
6	<b>2a</b> (5)	$\text{BBr}_3$ (2.8)	24 h	<b>1a</b> , 50%; unidentified products, 50%
7	<b>2a</b> (5)	$\text{HgCl}_2$ (3.1)	24 h	<b>1a</b> , 25%; <b>2a</b> , 75%
8	<b>2a</b> (1)	1% $\text{AgNO}_3$ -SBA-15 <sup>[b, 36a]</sup> (10)	20 min	<b>1a</b> , 30%; <b>2a</b> , 70%
9	<b>2a</b> (5)	1% $\text{AgNO}_3$ - $\text{SiO}_2$ <sup>[36b]</sup> (50)	1 h	<b>1a</b> , 100%
10	<b>2b</b> (5)	$\text{AgNO}_3$ (1.3)	18 min	<b>1b</b> , 100%
11	<b>2b</b> (10)	1% $\text{AgNO}_3$ - $\text{SiO}_2$ <sup>[36b]</sup> (40; 0.2 equiv Ag)	5 min	<b>1b</b> , 100%

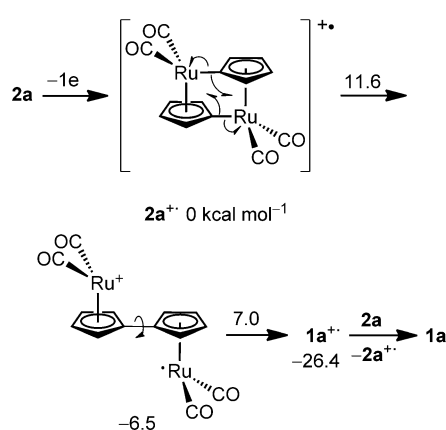
[a] Experimental: **2** in THF (1.0 mL) was treated with the catalyst candidate at RT and conversions monitored by thin-layer chromatography and <sup>1</sup>H NMR spectroscopy. For the runs with the various versions of  $\text{AgNO}_3$ , care was taken to exclude light. [b] Mesoporous silica; SBA = Santa Barbara Amorphous.



**Table 5.** Crystal data and structure refinement for complexes **1 b**, **2 b**, **7**, **9**, **10**, **21**, **25**, **27**, and **31**.

	<b>1 b</b>	<b>2 b</b>	<b>7</b>	<b>9</b>	<b>10</b>	<b>21</b>	<b>25</b>	<b>27</b>	<b>31</b>
formula	C <sub>30</sub> H <sub>40</sub> O <sub>4</sub> Ru <sub>2</sub>	C <sub>30</sub> H <sub>40</sub> O <sub>4</sub> Ru <sub>2</sub>	C <sub>30</sub> H <sub>40</sub> BF <sub>4</sub> I <sub>4</sub> O <sub>4</sub> Ru <sub>2</sub> ·CH <sub>2</sub> Cl <sub>2</sub>	C <sub>38</sub> H <sub>24</sub> O <sub>4</sub> Ru <sub>2</sub>	C <sub>18</sub> H <sub>12</sub> O <sub>8</sub> Ru <sub>2</sub>	C <sub>22</sub> H <sub>18</sub> O <sub>4</sub> Ru <sub>2</sub>	C <sub>30</sub> H <sub>40</sub> O <sub>4</sub> Os <sub>2</sub>	C <sub>30</sub> H <sub>40</sub> FeO <sub>4</sub> Ru	C <sub>14</sub> H <sub>8</sub> I <sub>2</sub> O <sub>4</sub> Ru <sub>2</sub>
F <sub>w</sub>	666.76	666.76	965.42	746.71	558.4	548.50	845.02	621.54	696.14
temperature [K]	125(2)	131(2)	298(2)	138(2)	168(2)	100(2)	100(2)	100(2)	139(2)
wavelength [Å]	0.71073	0.71073	0.71073	0.71073	0.71073	0.71073	0.71073	0.71073	0.71073
crystal system	monoclinic	monoclinic	monoclinic	triclinic	monoclinic	monoclinic	monoclinic	monoclinic	triclinic
space group	P2 <sub>1</sub> /c	P2 <sub>1</sub> /n	P2 <sub>1</sub> /n	P1	P2 <sub>1</sub> /c	P2 <sub>1</sub> /c	P2 <sub>1</sub> /n	P2 <sub>1</sub> /c	P1
a [Å]	13.412(1)	12.086(2)	17.5793(27)	10.0433(9)	17.5537(20)	19.8984(11)	12.1062(14)	13.3851(4)	6.3201(9)
b [Å]	12.746(1)	8.513(1)	10.0733(12)	11.4869(10)	13.8112(20)	8.5457(5)	8.5097(10)	12.4395(4)	6.7493(10)
c [Å]	17.401(1)	14.066(2)	22.1112(30)	13.5441(12)	15.4889(20)	12.0410(6)	14.0581(16)	17.5408(5)	11.1027(16)
α [°]	90	90	90	76.1310(10)	90	90	90	90	99.765(2)
β [°]	106.842(1)	100.142(2)	96.533(12)	89.3560(10)	101.307(11)	99.087(2)	100.539(2)	107.1990(10)	105.885(2)
γ [°]	90	90	90	77.3960(10)	90	90	90	90	101.830(2)
V [Å <sup>3</sup> ]	2847.1(4)	1424.7(3)	3890.1(17)	1479.0(2)	3682.2(15)	2021.82(19)	1423.8(3)	2790.01(15)	432.83(11)
Z	4	2	4	2	8	4	2	4	1
ρ <sub>calcd</sub> [g cm <sup>-3</sup> ]	1.556	1.554	1.65	1.677	2.01	1.802	1.971	1.480	2.671
μ(MoKα) [cm <sup>-1</sup> ]	1.09	1.09	17.3	10.63	16.5	15.18	89.48	10.94	53.22
R <sub>1</sub> [I > 2σ(I)]	0.0279	0.0242	0.0397 <sup>[a]</sup>	0.0262	0.0271 <sup>[a]</sup>	0.0251	0.0133	0.0260	0.0250
wR <sub>2</sub> (all data)	0.0688	0.0551	0.0542	0.0704	0.0266	0.0548	0.0322	0.0629	0.0491

[a] I > 3σ(I).



**Scheme 11.** One-electron-transfer catalysis by AgNO<sub>3</sub> in the conversion of **2 a** to **1 a**. Δ*H* (below the respective species) and Δ*H*<sup>‡</sup> values (above reaction arrows; DFT-PBE with plane-wave basis)<sup>[3]</sup> are relative to **2 a**<sup>•+</sup>(0).

Acros Organics)<sup>[36b]</sup> to generate the data of entry 11, Table 4. Ordinary chromatography silica (Fisher Scientific, grade 100) caused visible (blackening of a slurry) deterioration of **2 b** after 1 day, whereas its ultrapure version left it untouched for at least 8 days. To ascertain the level of activity retained by the used catalyst, it was filtered and re-exposed to a fresh batch of **2 b**, revealing much slower conversion to **1 b** (~95% in 24 h), while the solid acquired a greyish tinge. Leaching of the catalyst by solvent THF appeared unlikely, as the filtered solution of **1 b** could be converted back fully to **2 b** on irradiation. One notes in this connection that AgNO<sub>3</sub>-SiO<sub>2</sub> has been a chromatography staple for decades.<sup>[49]</sup>

The origin of catalyst vulnerability is probably related to the well-documented decomposition of AgNO<sub>3</sub>-SiO<sub>2</sub> to Ag metal and/or Ag silicates,<sup>[50]</sup> and it may also be associated with the mechanism of its action. For the latter, a reasonable working hypothesis, formulated in analogy to the one-electron-transfer

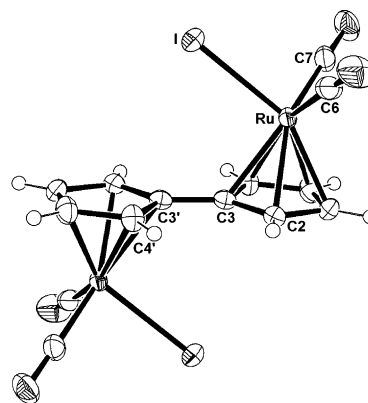


**Figure 8.** ORTEP rendition of **31** with thermal ellipsoids at 50% probability. The structure has inversion symmetry. Selected bond lengths [Å] and angles [°] in comparison to those of experimentally determined FvRu<sub>2</sub>(CO)<sub>4</sub>Cl<sub>2</sub> (in curly brackets):<sup>[2]</sup> Cp<sub>centroid</sub>-Ru 1.884 {1.874}, Ru1-C3 2.282(4) {2.256}, C3-C3' 1.457(8) {1.46}, Ru-I 2.7018(5) {2.413}, Ru-C6 1.893(5) {1.899}, Ru-C7 1.881(5) {1.897}, C3-C3'-Ru 124.2(4) {123.7}, C3-Ru-I 92.07(10) {92.9}, I-Ru-C6 91.09(14) {91.9}, I-Ru-C7 88.72(14) {90.4}, C6-Ru-C7 91.03(19) {91.2}, C2-C3-C3'-C4' -0.87 {-1.1}, Cp<sub>1plane</sub>-Cp<sub>2plane</sub> (fulvalene bend) 0 {0}.

catalysis pathway found for the quadricyclane-norbornadiene rearrangement<sup>[34]</sup> and supported by preliminary DFT calculations, is summarized in Scheme 11.

Unlike the thermal reversal of neutral **2 a**, for which the first (and endothermic) step (Cp-Cp coupling, Δ*H* = +18 kcal mol<sup>-1</sup>) requires an activation of 22.4 kcal mol<sup>-1</sup> and the subsequent CpRu rotation is rate determining (29.7 kcal mol<sup>-1</sup>), in the computed radical cation manifold the former is rate determining and considerably faster (Δ*H*<sup>‡</sup> = 11.8 kcal mol<sup>-1</sup>), in addition to being exothermic. In the hope to shed some light on the plausibility of Scheme 11, cyclic voltammetry measurements were executed with **2 a** and **b** in THF (see the Supporting Information). Unfortunately, although not unexpected in light of similar results with the parent complex **1 a** (*E*<sub>pa,FC</sub> =

0.50 V, suspected 2e process),<sup>[35,51]</sup> oxidation (**2a**,  $E_{pa,FC}=0.93$  V; **2b**,  $E_{pa,FC}=0.77$  V) proved to be irreversible, even at high sweep rates, precluding further analysis. Interestingly, however, all species exhibit values for  $E_{pa} > Ag^+$  (0.41 V),<sup>[52]</sup> suggesting that bulk oxidation of the system by  $AgNO_3$  is unlikely.

## Conclusion

We have presented a fairly comprehensive study of the scope and limitations of varying the ligand framework around the dinuclear core of  $FvRu_2$  in its function as a photothermal energy-storage entity. DFT calculations reveal a system, in which the  $\Delta H_{storage}$  values seem remarkably impervious to steric and electronic substituent effects on the Fv ligand. This outcome is likely the result of small and/or cancelling influences on the relative energies of individual pairs of parent and photoisomer structures. Experimentally, a number of derivatives of  $FvRu_2(CO)_4$  were shown to complete successfully the photoisomerization–thermal reversal cycle, tolerating altered Fv ligands in the form of tetra-*tert*-butyl (in the  $\beta$ -positions; **1b**), di(methoxycarbonyl) (**10** and five isomers), cyclopentenone and cyclopentadienyl ( $\alpha$ , **14** and **18**, or  $\beta$ , **15** and **19**), and indenyl (**20**). Exchange of CO by electron-donating species seems feasible, as demonstrated by the mono- $PEt_3$  complex **22**. Failures include 1,1',3,3'-tetra-*tert*-butyl (**3**), 1,2,2',3'-tetraphenyl (**9**), diiron (**28**), diosmium (**24**), mixed iron-ruthenium (**27**), dimolybdenum (**29**), and ditungsten (**30**) derivatives. An extensive screen of potential catalysts for the thermal reversal identified  $AgNO_3$  as best for this purpose, particularly when anchored on  $SiO_2$ , although catalyst decomposition remains a problem.

## Experimental Section

### General methods

Unless otherwise indicated, all manipulations were conducted under purified  $N_2$ , for air-sensitive compounds either in a Vacuum Atmospheres Inc. glovebox or using standard Schlenk vacuum line techniques. Ether solvents were distilled from either potassium or sodium benzophenone ketyl immediately prior to use; hexanes,  $C_6H_6$ , toluene, and xylenes from calcium hydride or benzophenone ketyl; and  $CH_2Cl_2$  from  $CaCl_2$  or  $P_2O_5$ . Chromatography solvents were deoxygenated by purging with a stream of  $N_2$ . Photoreactions were performed in Pyrex vessels, either employing GE ELH 300 W projector or near-UV lamps of primary output between 325 and 375 nm ( $\lambda_{max}$  at 350 nm). As wavelength cut-offs, aqueous  $NaNO_2$  (75% w/v) or Newport Corporation 65CGA-400 or -550 filters were employed. Melting points were observed in sealed glass capillaries under  $N_2$  on a Büchi or a Thomas–Hoover Unimelt melting point apparatus and are uncorrected.  $^1H$  NMR spectra were obtained on Bruker AV-300, AVB-400, AV-500, and AVQ-400 spectrometers, and  $^{13}C$  NMR data on AVQ-400, DRX-500, and AV-600 instruments. All chemical shifts are referenced relative to residual solvent.  $^{31}P$  NMR spectra were recorded on an AVQ-400 machine, and chemical shifts are quoted relative to 85%  $H_3PO_4$ . IR spectra were measured on PerkinElmer Model 681 and Spectrum 100 FT-IR spectrophotometers, and UV/Vis absorptions on PerkinElmer Lambda 35 and Hewlett–Packard 8450A UV/Vis diode array systems. Kinetics for thermal reversions were followed on an Agilent 8453 UV/Vis spectrometer containing an Agilent 8909A Peltier temperature con-

trol unit. GC/MS analyses were performed on an Agilent 6890 Series GC system equipped with an Agilent 5973 mass selective detector and a HP-5 column (30 m  $\times$  0.25 mm  $\times$  0.25  $\mu$ m). Mass spectral data were provided by the UCB Mass Spectrometry Laboratory and collected on AEI-MS12, Finnigan 4000, or Kratos MS50 instruments. Because the natural isotopic distribution of Ru resulted in broad peak envelopes, only the major peak for each fragment is reported. Elemental analyses were carried out by the UCB Micro-analytical Laboratory. Cyclic voltammetry experiments were performed using a BASi EC Epsilon electrochemical analyzer.

### (1,1',3,3'-Tetra-*tert*-butylfulvalene)tetracarbonyldiruthenium (4)

To a boiling solution of  $Ru_3(CO)_{12}$  (50 mg, 0.078 mmol) in DME (10 mL) was added a solution of 1,1',3,3'-tetra-*tert*-butylfulvalene (**3**) (80 mg, 0.23 mmol) in heptane (10 mL) over 2 h. The resulting dark red-orange solution was boiled for an additional 30 h, cooled, and filtered through activity III alumina, eluting with  $CH_2Cl_2$ . The solvent was evaporated and the residue chromatographed on activity III alumina. Elution with  $Et_2O$ /hexanes (1:9) gave first a red band containing unreacted ligand (30 mg, 38% recovery), followed by a yellow band. After removal of the volatiles, the residue was taken up in a minimum of hexanes and the solution cooled slowly to  $-78^\circ C$  to afford yellow crystals of analytically pure **4** (40 mg, 42%). M.p.  $196^\circ C$  (dec.).  $^1H$  NMR (300 MHz,  $CDCl_3$ ):  $\delta=5.97$  (d,  $J=2.2$  Hz, 2H), 3.24 (d,  $J=2.2$  Hz, 2H), 1.27 (s, 18H), 1.17 ppm (s, 18H);  $^{13}C$  NMR ( $CDCl_3$ ):  $\delta=208.2$ , 204.6, 119.1, 117.8, 89.3, 86.1, 76.6, 33.7, 31.5, 31.1, 30.3 ppm; IR ( $CH_2Cl_2$ ):  $\tilde{\nu}_{CO}=2011$ ,  $1942\text{ cm}^{-1}$ ; UV/Vis (THF):  $\lambda_{max}$  ( $\log \epsilon$ ) = 239 (4.17), 274 (4.00), 331 (3.78), 402 nm (sh) (3.23); MS (70 eV):  $m/z$  (%): 667 [ $M^+$ ] (36), 550 [ $M^+ - 4CO$ ] (36), 57 [ $CMe_3^+$ ] (100); elemental analysis calcd (%) for  $C_{30}H_{40}O_4Ru_2$ : C 54.04, H 6.05; found: C 53.79, H 5.99.

### (1,1',3,3'-Tetra-*tert*-butylfulvalene)tetracarbonyldiruthenium dichloride (5)

A solution of **4** (50 mg, 0.075 mmol) in  $THF/CCl_4$  (1:1, 50 mL) was irradiated (350 nm, Rayonet) for 1 h. The solvent was removed and the residue filtered through activity III alumina, eluting with  $CH_2Cl_2$ . Crystallization from  $CH_2Cl_2$ /hexanes gave yellow crystals of **5** (35 mg, 63%). M.p.  $177^\circ C$  (dec.).  $^1H$  NMR (300 MHz,  $CDCl_3$ ):  $\delta=6.70$  (d,  $J=2.0$  Hz, 2H), 5.48 (d,  $J=2.0$  Hz, 2H), 1.33 (s, 18H), 1.08 ppm (s, 18H);  $^{13}C$  NMR ( $CDCl_3$ ):  $\delta=197.0$ , 195.8, 126.0, 104.9, 96.2, 93.4, 85.8, 34.1, 32.2, 31.0, 30.2 ppm; IR ( $CH_2Cl_2$ ):  $\tilde{\nu}_{CO}=2061$ ,  $1999\text{ cm}^{-1}$ ; UV/Vis (THF):  $\lambda_{max}$  ( $\log \epsilon$ ) = 303 (3.70), 400 nm (2.85); FAB-MS (NBA):  $m/z$ : 703 [ $M^+ - Cl$ ], 675 [ $M^+ - Cl, -CO$ ]; elemental analysis calcd (%) for  $C_{30}H_{40}Cl_2O_4Ru_2$ : C 48.85, H 5.47, Cl 9.6; found: C 49.08, H 5.53, Cl 9.82.

### (1,1',3,3'-Tetra-*tert*-butylfulvalene)tetracarbonyldiruthenium diiodide (6)

Ligand **3** (600 mg, 1.70 mmol) in glyme (20 mL) was added to  $Ru_3(CO)_{12}$  (746 mg, 1.17 mmol) in boiling glyme (40 mL) over 20 min and the mixture heated for another 24 h. After cooling to RT, the orange solution was passed through alumina, eluting with  $CH_2Cl_2$ , and the solvent replaced with THF (5 mL). Addition of  $I_2$  (0.50 g, 1.97 mmol) in THF (3 mL) was followed by treatment with aqueous  $Na_2S_2O_3$ , extraction with  $Et_2O$ , and filtering through alumina, eluting with  $Et_2O$ . The liquid was mixed with heptane (10 mL) and subjected to partial rotary evaporation to cause precipitation of **6** (780 mg, 50%) as orange crystals. M.p.  $224\text{--}226^\circ C$  (dec.).  $^1H$  NMR (300 MHz,  $CDCl_3$ ):  $\delta=6.21$  (d,  $J=2.1$  Hz, 2H), 5.51 (d,  $J=$

2.1 Hz, 2H), 1.33 (s, 18H), 1.21 ppm (s, 18H);  $^{13}\text{C}$  NMR ( $\text{CDCl}_3$ ):  $\delta = 196.32, 196.13, 122.3, 109.6, 97.4, 94.4, 88.1, 33.8, 33.2, 31.5, 30.9$  ppm; IR ( $\text{CH}_2\text{Cl}_2$ ):  $\tilde{\nu}_{\text{CO}} = 2050, 1992$   $\text{cm}^{-1}$ ; UV/Vis (THF):  $\lambda_{\text{max}}$  ( $\log \epsilon$ ) = 312 (4.02), 416 nm (3.09); elemental analysis calcd (%) for  $\text{C}_{30}\text{H}_{40}\text{I}_2\text{O}_4\text{Ru}_2$ : C 39.14, H 4.38; found: C 39.30, H 4.47.

### Iodonium salt 7

Diiodide **6** (250 mg, 0.27 mmol) in  $\text{CH}_2\text{Cl}_2$  (3 mL) was treated with  $\text{AgBF}_4$  (53 mg, 0.27 mmol). After 20 min, the yellow  $\text{AgI}$  precipitate was filtered off and the orange solution mixed with ether to give **7** (202 mg, 85%) as orange crystals, recrystallized from  $\text{CH}_2\text{Cl}_2/\text{hexanes}$ .  $^1\text{H}$  NMR (300 MHz,  $\text{CDCl}_3$ ):  $\delta = 6.03$  (d,  $J = 2.3$  Hz, 2H), 5.18 (d,  $J = 2.3$  Hz, 2H), 1.40 (s, 18H), 1.34 ppm (s, 18H); IR ( $\text{CH}_2\text{Cl}_2$ ):  $\tilde{\nu}_{\text{CO}} = 2051, 2011$   $\text{cm}^{-1}$ ; elemental analysis calcd (%) for  $\text{C}_{30}\text{H}_{40}\text{BF}_4\text{IO}_4\text{Ru}_2$ : C 40.92, H 4.58, I 14.41; found: C 40.66, H 4.48, I 14.49.

### (1,2,2',3'-Tetraphenylfulvalene)tetracarbonyldiruthenium (9)

To a dried Schlenk flask under Ar was added freshly prepared 1,2-diphenyl-1,3-cyclopentadiene (201.5 mg, 0.923 mmol) and THF (30 mL). After cooling to  $-78^\circ\text{C}$ , BuLi in hexanes (2.5 M, 0.37 mL, 0.925 mmol) was added dropwise, followed by stirring at  $-78^\circ\text{C}$  for 10 min and slow warming to RT over 12 h. The resulting solution was cooled to  $0^\circ\text{C}$  and  $\text{CuCl}_2$  (149.6 mg, 1.11 mmol) added in one portion. An immediate color change to black-green occurred, changing to brown-black over time. After being stirred for 30 min at RT, the mixture was filtered through celite, washed with  $\text{H}_2\text{O}$ , then satd aqueous  $\text{NaHCO}_3$ , followed by satd aqueous  $\text{NaCl}$ , and subsequently dried over anhydrous  $\text{MgSO}_4$ . The solvent was removed and the mixture loaded into a resealable Schlenk bomb containing  $\text{Ru}_3\text{CO}_{12}$  (295.0 mg, 0.461 mmol) and dried degassed toluene (20 mL). The vessel was sealed, heated at  $120^\circ\text{C}$  for 12 h, allowed to cool to RT, and the solvent removed under vacuum to yield **9** (95.4 mg, 27.6%) as a yellow solid.  $^1\text{H}$  NMR (400 MHz,  $\text{CDCl}_3$ ):  $\delta = 7.67$  (bs, 1H), 7.36–7.30 (m, 5H), 7.25–7.17 (m, 8H), 7.17–7.10 (m, 5H), 6.60 (bs, 1H), 5.82 (d,  $J = 2.8$  Hz, 1H), 4.28 (d,  $J = 2.5$  Hz, 1H), 3.96 (d,  $J = 2.9$  Hz, 1H), 3.51 ppm (d,  $J = 2.3$  Hz, 1H);  $^{13}\text{C}$  NMR (125 MHz,  $\text{CDCl}_3$ ):  $\delta = 205.9, 205.4, 205.2, 205.0, 132.79, 132.73$  (br), 132.6, 132.5 (br), 131.6, 131.5, 130.5, 130.5, 130.2, 129.0 (br), 128.67, 128.60 (br), 128.44, 128.41, 128.3, 128.2, 128.15, 128.14, 112.7, 111.7, 110.3, 104.8, 92.0, 91.8, 87.1, 79.6, 79.3, 75.7 ppm; IR (film):  $\tilde{\nu}_{\text{CO}} = 2013, 1957, 1938, 1607, 1577, 1493, 1449, 1431, 1074, 910, 844, 764, 734, 698, 608, 573, 548, 523$   $\text{cm}^{-1}$ ; UV/Vis (THF):  $\lambda_{\text{max}}$  (A) = 260 sh (1.02), 349 (0.41), 399 sh (0.20), end absorption to 480 nm; MS (70 eV):  $m/z$  (%): 748 [ $M^+$ ] (60), 720 [ $M^+ - \text{CO}$ ] (20), 692 [ $M^+ - 2\text{CO}$ ] (60), 664 [ $M^+ - 3\text{CO}$ ] (50), 318 [ $\text{Ph}_2\text{CpRu}^+$ ] (100).

### (Dimethyl fulvalene-1,1'-dicarboxylate)tetracarbonyldiruthenium (10)

For a detailed experimental description, see the Supporting Information. Spectral data:  $^1\text{H}$  NMR (500 MHz,  $[\text{D}_8]\text{THF}$ ; see structure for numbering scheme):  $\delta = 6.46$  (dd,  $J_{2,3} = 3.0, J_{2,4} = 2.0$  Hz, 2H; H2), 5.82 (t,  $J_{2,3} = 3.4 = 3.0$  Hz, 2H; H3), 4.90 (dd,  $J_{3,4} = 3.1, J_{2,4} = 2.0$  Hz, 2H; H4), 3.62 ppm (s, 6H;  $\text{CH}_3$ );  $^{13}\text{C}$  NMR ( $[\text{D}_8]\text{THF}$ ):  $\delta = 205.7$  (RuCO), 205.5 (RuCO), 166.7 (OCO), 93.9 (C2), 92.5 ( $\text{C}_{\text{quat}}$ ), 90.8 ( $\text{C}_{\text{quat}}$ ), 89.4, 84.8 (C3, C4), 53.0 ppm ( $\text{CH}_3$ ); IR (KBr):  $\tilde{\nu} = 3152, 3130, 2959, 20171, 1979, 1955, 1941, 1727, 1449, 1426, 1379, 1336, 1245, 1200, 1160, 1122, 1073, 1044, 976, 891, 819, 798, 777$   $\text{cm}^{-1}$ ; UV/Vis (THF):  $\lambda_{\text{max}}$  ( $\log \epsilon$ ) = 277 (3.74), 335 (3.45), 418 nm (sh) (2.78); MS (70 eV):  $m/z$  (%): 558 [ $M^+$ ] (25), 530 [ $M^+ - \text{CO}$ ] (25), 502 [ $M^+ - 2\text{CO}$ ] (52), 474 [ $M^+ - 3\text{CO}$ ] (75), 446 [ $M^+ - 4\text{CO}$ ] (66), 416 (63), 387 (59), 331 (100),

328 (91); elemental analysis calcd (%) for  $\text{C}_{18}\text{H}_{12}\text{O}_8\text{Ru}_2$ : C 38.71, H 2.17; found: C 38.98, H 2.21.

### Photoisomerization of 10 to 11

In an NMR tube, a sample of **10** (5 mg) in  $[\text{D}_8]\text{THF}$  was irradiated for 3 h using a Sylvania ELH 300 W slide projector lamp, causing near complete conversion to **11**.  $^1\text{H}$  NMR (500 MHz,  $[\text{D}_8]\text{THF}$ ; see structure for numbering scheme):  $\delta = 6.17$  (dd,  $J_{2,3} = 3.1, J_{2,4} = 1.9$  Hz, 2H; H2), 5.68 (dd,  $J_{2,3} = 3.0, J_{3,4} = 2.5$  Hz, 2H; H3), 4.85 (t,  $J_{3,4} = 2.4 = 2.2$  Hz, 2H; H4), 3.70 ppm (s, 6H;  $\text{CH}_3$ );  $^{13}\text{C}$  NMR ( $[\text{D}_8]\text{THF}$ ):  $\delta = 201.6, 200.1$  (RuCO), 166.9 (OCO), 101.2 ( $\text{C}_{\text{quat}}$ ), 99.7, 94.5, 93.3, 90.7 (C1, C4, C2, C3, C4a), 52.2 ppm ( $\text{CH}_3$ ); MS (70 eV):  $m/z$  (%): 558 [ $M^+$ ] (26), 530 (43), 502 (43), 474 (79), 446 (72), 416 (49), 387 (45), 331 (100), 328 (72).

### Photoisomerization of 12 to 14

A yellow solution of **12** (75 mg, 0.14 mmol) in THF (100 mL) was irradiated in a Pyrex vessel with a GE ELH 300 W projector lamp at RT for 8 h. After evaporation of solvent, the residue was chromatographed on alumina (50 g), eluting with  $\text{Et}_2\text{O}/\text{hexane}$  (7:3), to give **14** (55 mg, 73%) as colorless crystals. M.p.  $249\text{--}250^\circ\text{C}$  (dec.; from  $\text{Et}_2\text{O}/\text{hexane}$ ; the sample isomerizes to **12** at  $152\text{--}154^\circ\text{C}$ ).  $^1\text{H}$  NMR (400 MHz,  $[\text{D}_8]\text{THF}$ ):  $\delta = 6.50$  (t,  $J = 1.8$  Hz, 1H), 5.95 (dd,  $J = 3.1, 1.8$  Hz, 1H), 5.74 (t,  $J = 2.7$  Hz, 1H), 5.71 (td,  $J = 2.8, 1.5$  Hz, 1H), 5.51 (m, 1H), 4.92 (dd,  $J = 2.6, 1.6$  Hz, 1H), 4.90 (dd,  $J = 2.3, 1.9$  Hz, 1H), 4.61 (dt,  $J = 2.5, 1.6$  Hz, 1H), 3.00 (m, 1H), 2.74 (m, 1H), 2.38 (t,  $J = 3.4$  Hz, 1H), 2.37 ppm (t,  $J = 3.6$  Hz, 1H);  $^{13}\text{C}$  NMR ( $[\text{D}_8]\text{THF}$ ):  $\delta = 207.0, 203.0, 202.0, 201.7, 201.4, 171.2, 132.1, 111.3, 99.3, 98.9, 96.2, 94.2, 92.7, 91.4, 89.1, 86.8, 84.8, 35.6, 33.7$  ppm; IR ( $\text{CH}_2\text{Cl}_2$ ):  $\tilde{\nu} = 2014, 1969, 1711, 1683, 1606$   $\text{cm}^{-1}$ ; UV/Vis (THF):  $\lambda_{\text{max}}$  ( $\log \epsilon$ ) = 302 nm (sh) (3.87); MS (70 eV):  $m/z$  (%): 523 [ $M^+$ ] (51), 494 (14), 466 (58), 438 (51), 409 (36), 380 (100), 353 (37); elemental analysis calcd (%) for  $\text{C}_{19}\text{H}_{12}\text{O}_5\text{Ru}_2$ : C 43.68, H 2.32; found: C 43.18, H 2.45.

### Photoisomerization of 13 to 15

A yellow solution of **13** (103 mg, 0.20 mmol) in THF (100 mL) was irradiated in a Pyrex vessel with a GE ELH 300 W projector lamp at RT for 2 d. After evaporation of solvent, the residue was chromatographed on silica gel (75 g), eluting with  $\text{Et}_2\text{O}$ , to give starting material **13** (28 mg, 27%), followed by **15** (41 mg, 54% based on recovered **13**) as ivory crystals. M.p.  $239\text{--}240^\circ\text{C}$  (dec.; from  $\text{Et}_2\text{O}/\text{hexane}$ ; the sample isomerizes to **13** at  $156\text{--}157^\circ\text{C}$ ).  $^1\text{H}$  NMR (300 MHz,  $\text{CDCl}_3$ ):  $\delta = 6.20$  (t,  $J = 1.6$  Hz, 1H), 5.78 (dd,  $J = 2.1, 2.0$  Hz, 1H), 5.42 (m, 2H), 5.10 (t,  $J = 1.7$  Hz, 1H), 4.78 (m, 2H), 4.65 (dd,  $J = 2.0, 1.8$  Hz, 1H), 2.72 (m, 2H), 2.49 ppm (m, 2H);  $^{13}\text{C}$  NMR ( $[\text{D}_8]\text{THF}$ ):  $\delta = 206.8, 201.8$  (2C), 201.3, 200.9, 167.0, 128.1, 107.1, 97.6, 96.8, 96.4, 96.2, 92.08, 92.06, 91.7, 88.9, 85.4, 35.2, 25.9 ppm; IR ( $\text{CH}_2\text{Cl}_2$ ):  $\tilde{\nu} = 2021, 1970, 1710, 1680, 1605$   $\text{cm}^{-1}$ ; UV/Vis (THF):  $\lambda_{\text{max}}$  ( $\log \epsilon$ ) = 283 (sh) (3.94), 342 nm (3.69); elemental analysis calcd (%) for  $\text{C}_{19}\text{H}_{12}\text{O}_5\text{Ru}_2$ : C 43.68, H 2.32; found: C 43.48, H 2.38.

### Photoisomerization of 16 to 18

A yellow solution of **16** (18 mg, 0.023 mmol) in  $[\text{D}_8]\text{THF}$  (0.6 mL) in a sealed NMR tube maintained at  $0^\circ\text{C}$  was exposed to a GE ELH 300 W projector lamp at RT for 8 h, during which the solution turned colorless. An  $^1\text{H}$  NMR spectrum of the sample showed  $>90\%$  conversion to **18**. The sample was filtered through a plug of silica gel, the latter was subsequently washed with  $\text{Et}_2\text{O}$ . The volatiles were removed in vacuo to give **18** (16 mg, 88.9%) as light tan crystals. M.p.  $240\text{--}243^\circ\text{C}$  (dec.; from  $\text{Et}_2\text{O}/\text{hexane}$ ; the sample

isomerizes to **16** at 189 °C). <sup>1</sup>H NMR (400 MHz, [D<sub>8</sub>]THF): δ = 5.97 (td, *J* = 2.8, 1.7 Hz, 1H), 5.65 (td, *J* = 2.8, 1.7 Hz, 1H), 5.60 (m, 2H), 5.57 (m, 1H), 5.55 (m, 1H), 5.51 (td, *J* = 2.8, 1.7 Hz, 1H), 5.45 (td, *J* = 2.8, 1.7 Hz, 1H), 4.86 (dd, *J* = 3.8, 1.6 Hz, 1H), 4.80 (dd, *J* = 3.8, 1.6 Hz, 1H), 4.75 ppm (t, *J* = 2.1 Hz, 1H); <sup>13</sup>C NMR ([D<sub>8</sub>]THF): δ = 202.5, 202.0, 201.63, 201.60, 195.2, 110.2, 104.7, 97.7, 97.6, 97.0, 96.9, 92.6, 92.1, 91.5, 91.4, 90.8, 89.5, 84.9, 84.6, 83.6 ppm; IR (CH<sub>2</sub>Cl<sub>2</sub>):  $\tilde{\nu}$  = 2014, 1967, 1931 cm<sup>-1</sup>; UV/Vis (THF):  $\lambda_{\text{max}}$  (log  $\epsilon$ ) = 262 (3.81), 288 nm (sh) (3.68); MS (70 eV): *m/z* (%): 778 [*M*<sup>+</sup>] (22), 750 (7), 722 (19), 694 (19), 666 (55), 638 (32), 608 (52), 578 (93), 70 (100); elemental analysis calcd (%) for C<sub>22</sub>H<sub>11</sub>O<sub>7</sub>ReRu<sub>2</sub>: C 34.07, H 1.43; found: C 34.12, H 1.14.

### Photoisomerization of 17 to 19

A solution of **17** (20 mg, 0.026 mmol) in [D<sub>8</sub>]THF (0.6 mL) in a sealed NMR tube maintained at 0 °C was exposed to a GE ELH 300 W projector lamp at RT for 24 h. Chromatography on silica gel (50 g), eluting with hexane/Et<sub>2</sub>O (8:2), gave first starting material **17** (5 mg, 25%), followed by **19** (10 mg, 67% based on recovered **17**) as colorless crystals. M.p. 270–272 °C (dec.; from Et<sub>2</sub>O/hexane; the sample isomerizes to **17** at 190 °C). <sup>1</sup>H NMR (400 MHz, C<sub>6</sub>D<sub>6</sub>): δ = 4.91 (dd, *J* = 2.4, 1.7 Hz, 1H), 4.70 (m, 1H), 4.67 (m, 2H), 4.63 (dt, *J* = 2.7, 1.8 Hz, 1H), 4.60 (dt, *J* = 2.7, 1.8 Hz, 1H), 4.28 (m, 1H), 4.25 (m, 2H), 4.05 (m, 1H), 4.03 ppm (m, 1H); IR (CH<sub>2</sub>Cl<sub>2</sub>):  $\tilde{\nu}$  = 2016, 1968, 1931 cm<sup>-1</sup>; UV/Vis (THF):  $\lambda_{\text{max}}$  (log  $\epsilon$ ) = 268 sh (3.71), 318 nm (sh) (3.27); MS (70 eV): *m/z* (%): 778 [*M*<sup>+</sup>] (20), 722 (12), 694 (41), 666 (41), 636 (39), 610 (27), 578 (83), 57 (100); elemental analysis calcd (%) for C<sub>22</sub>H<sub>11</sub>O<sub>7</sub>ReRu<sub>2</sub>: C 34.07, H 1.43; found: C 34.09, H 1.23.

### Photoisomerization of 20 to 21

A Schlenk flask containing orange **20** (60 mg, 0.11 mmol) in toluene (10 mL) was thermostated at 25 °C by a circulating bath (*i*PrOH) and irradiated for 8 h with an Eiko 300 W projector lamp through an aqueous NaNO<sub>2</sub> filter (75% w/v; 400 nm cutoff). After removal of solvent, the residue was purified by column chromatography on alumina, eluting with petroleum ether/CH<sub>2</sub>Cl<sub>2</sub> (8:1), to deliver **21** (37 mg, 62%) as an ivory-colored powder. <sup>1</sup>H NMR (500 MHz, CDCl<sub>3</sub>): δ = 7.38 (AA'm, 2H), 7.04 (BB'm, 2H), 5.38 (s, 1H), 5.35 (m, 2H), 4.82 (t, *J* = 1.8 Hz, 1H), 4.66 (t, *J* = 1.9 Hz, 1H), 1.17 ppm (s, 9H); <sup>1</sup>H NMR (600 MHz, [D<sub>8</sub>]THF; see structure for numbering scheme): δ = 7.43 (AA'm, 2H; H10, H11), 7.04 (BB'm, 2H; H9, H12), 5.57 (t, *J* = 2.1 Hz, 1H; H5), 5.50 (brs, 1H; H7), 5.47 (brs, 1H; H14), 4.98 (t, *J* = 1.8 Hz, 1H; H2), 4.77 (t, *J* = 2.0 Hz, 1H; H-3), 1.19 ppm (s, 9H, CH<sub>3</sub>); <sup>13</sup>C NMR ([D<sub>8</sub>]THF): δ = 203.3, 202.4, 200.9, 200.8 (RuCO), 131.9 (C4), 126.47 (C9), 126.43 (C12), 122.64 (C10), 122.61 (C11), 115.4 (C8), 115.34 (C13), 94.6 (C2), 93.7 (C3), 89.6 (C5), 89.5 (C7), 89.32 (C6), 89.30 (C14), 85.8 (C1), 32.4 (CH<sub>3</sub>), 31.6 ppm (CCH<sub>3</sub>); IR (crystal):  $\tilde{\nu}$  = 2920, 2851, 2000, 1958, 1941, 1740, 1463, 1368 cm<sup>-1</sup>; UV/Vis (hexane):  $\lambda_{\text{max}}$  (log  $\epsilon$ ) = 242 (4.10), 299 (3.59), 357 nm (3.49); MS (EI): *m/z* (%): 550 [*M*<sup>+</sup>] (40), 522 (39), 494 (66), 464 (45), 433 (78), 217 (100); HRMS (EI): *m/z* calcd for C<sub>22</sub>H<sub>18</sub>O<sub>4</sub>Ru<sub>2</sub>: 549.9292 [*M*<sup>+</sup>]; found: 549.9280.

### Photoisomerization of 22 to 23

A J. Young NMR tube containing **22** (5 mg) in degassed C<sub>6</sub>D<sub>6</sub> (0.5 mL), kept at 20 °C by a circulating bath (*i*PrOH) and shielded by a Newport Corporation photo filter 65CGA-400, was exposed to a projector lamp for 2 h. <sup>1</sup>H NMR spectroscopy revealed complete conversion. After removing the solvent, pure **23** was obtained as an ivory solid. M.p. 120–130 °C (dec.). <sup>1</sup>H NMR (600 MHz, C<sub>6</sub>D<sub>6</sub>): δ =

4.88 (Am, 1H), 4.87 (Bm, 1H), 4.81 (dd, *J* = 3.6, 1.8 Hz, 1H), 4.66 (dd, *J* = 3.6, 1.8 Hz, 1H), 4.63 (brs, 1H), 4.58 (brs, 1H), 4.14 (dd, *J* = 3.6, 1.8 Hz, 1H), 4.10 (td, *J* = 3.6, 1.8 Hz, 1H), 1.27 (dq, *J* = 22.8, 7.8 Hz, 3H), 1.19 (dq, *J* = 22.8, 7.8, 1.8 Hz, 3H), 0.69 ppm (dt, *J* = 15.6, 7.8 Hz, 9H); <sup>13</sup>C NMR (C<sub>6</sub>D<sub>6</sub>): δ = 205.7 (d, *J* = 17.7 Hz), 202.7, 202.2, 98.5, 96.5 (d, *J* = 12.8 Hz), 93.8 (d, *J* = 10.2 Hz), 93.5 (d, *J* = 3.2 Hz), 92.9, 90.0, 89.8, 86.7, 86.1, 75.9, 21.9 (d, *J* = 27.6 Hz), 7.83 ppm; <sup>31</sup>P NMR (170 MHz, C<sub>6</sub>D<sub>6</sub>): δ = 47.28 ppm; IR (crystal):  $\tilde{\nu}$  = 2002, 1936, 1900, 1870, 1824, 1457, 1417, 1331, 1105, 1032, 1003, 858, 800, 767, 736 cm<sup>-1</sup>; UV/Vis (THF):  $\lambda_{\text{max}}$  (log  $\epsilon$ ) = 282 (3.70), 325 (sh) (3.35), 430 nm (sh) (2.73); HRMS (EI): *m/z* calcd for C<sub>19</sub>H<sub>23</sub>O<sub>3</sub>PRu<sub>2</sub>: 533.9472; found: 533.9494.

### (2,2',3,3'-Tetra-*tert*-butylfulvalene)tetracarbonyliron-ruthenium (27)

The following procedures, including chromatography, were executed all under Ar. *o*-Xylene (65 mL), followed by Fe(CO)<sub>5</sub> (0.20 mL, 1.55 mmol), was injected via syringe into a round-bottom flask charged with **26** (550 mg, 1.55 mmol) and Ru<sub>3</sub>(CO)<sub>12</sub> (330 mg, 0.52 mmol). The solution was heated to reflux for 17 h, cooled to RT, filtered through alumina, and the volatiles were removed to furnish a mixture of complexes **27**, **28**, and **1b** in the ratio = 1:1:1.6 (<sup>1</sup>H NMR). Column chromatography on alumina, eluting with petroleum ether/CH<sub>2</sub>Cl<sub>2</sub> (3:1), provided **27**, **28**, and **1b** (2:1:5.3, 510 mg). The mixture was dissolved in toluene (20 mL), irradiated with a projector lamp until all of **1b** had been converted to **2b**, the solvent removed, the residue redissolved in CH<sub>2</sub>Cl<sub>2</sub>, and the solution filtered through alumina, eluting with petroleum ether/Et<sub>2</sub>O (10:1) to afford, after removing the solvent, **2b** as a colorless solid (403 mg, 39%), followed by **27** (145 mg, 15%) as a red solid. M.p. 140–160 °C (dec.; from petroleum ether/Et<sub>2</sub>O). <sup>1</sup>H NMR (600 MHz, [D<sub>8</sub>]THF): δ = 4.36 (s, 2H), 3.89 (s, 2H), 1.43 (s, 18H), 1.42 ppm (s, 18H); <sup>13</sup>C NMR ([D<sub>8</sub>]THF): δ = 122.3, 116.4, 87.3, 84.6, 78.8, 79.9, 33.4, 32.9, 32.2, 29.6 ppm (FeCO could not be detected); IR (crystal):  $\tilde{\nu}$  = 2960, 2922, 2854, 1992, 1944, 1926, 1899, 1365, 1256, 1021, 997, 860, 800 cm<sup>-1</sup>; UV/Vis (THF):  $\lambda_{\text{max}}$  (log  $\epsilon$ ) = 292 (sh) (3.99), 335 (sh) (3.72), 388 (3.63), 485 nm (sh) (3.03); HRMS (ESI): *m/z* calcd for C<sub>30</sub>H<sub>41</sub>FeO<sub>4</sub>Ru: 623.1392; found: 623.1414.

### Crystal structure determinations

Complexes **1b**, **2b**, **9**, **21**, **25**, **27**, and **31**: X-ray intensity data were recorded on a Bruker SMART 1000 CCD area detector<sup>[50]</sup> with graphite monochromated MoK $\alpha$  radiation ( $\lambda$  = 0.71073 Å). Data were integrated by the program SAINT<sup>[54]</sup> and corrected for Lorentz and polarization effects. They were analyzed for agreement and possible absorption using XPREP<sup>[55]</sup>. An empirical absorption correction based on comparison of redundant and equivalent reflections was applied using SADABS<sup>[56]</sup>. The structures were solved by direct methods<sup>[57]</sup> and expanded using Fourier techniques<sup>[58]</sup>. The structures of **7** (1985) and **10** (1990) are dated and not available in cif format. Complete details of their structural determinations (on an Enraf-Nonius CAD-4 diffractometer) and topological details are provided in the Supporting Information.

CCDC 1010442 (**1b**), 1010446 (**2b**), 1010448 (**9**), 1010443 (**21**), 1010444 (**25**), 1010445 (**27**), and 1010447 (**31**) contain the supplementary crystallographic data for this paper. These data can be obtained free of charge from The Cambridge Crystallographic Data Centre via [www.ccdc.cam.ac.uk/data\\_request/cif](http://www.ccdc.cam.ac.uk/data_request/cif).



## Acknowledgements

We acknowledge support from the National Science Foundation through CHE-1213135 (C.B.H.), CHE-0907800 (K.P.C.V.), the Nano-scale Science and Engineering Center for Scalable and Integrated NanoManufacturing (NSEC SINAM CMMI-0751621; D.C. and A.M.), and a graduate research fellowship (J.P.L.); the Advanced Research Projects Agency-Energy (ARPA-E), US Department of Energy (DEAR0000180; J.C.G.); the Alfred P. Sloan Foundation for a faculty fellowship (R.A.S.); the Alexander von Humboldt Foundation for a Feodor Lynen Research Fellowship (N.H.); and the Danish Research Council (K.M.-P.; 09-066585/FNU), the Chalmers Materials and Energy Areas of Advance (K.M.-P. and K.B.), the Swedish Research Council (K.M.-P.), and China Scholar Council (J.G.) for postdoctoral funds. This work was executed under the auspices of the Sustainable Products and Solutions Program at UC Berkeley. We are indebted to the Molecular Graphics and Computation Facility at UC Berkeley for assistance (NSF CHE-0840505, CHE-0233882) and to the National Energy Research Scientific Computing Center for the use of its resources, backed by the Office of Science of the US Department of Energy under Contract No. DE-AC02-05CH11231. S.C.N. is grateful for a Vietnam International Education Development (VIED) graduate research fellowship. Cyclic voltammetry experiments benefited from the help of Dr. Han Sen Soo and Professor C. Chang at UC Berkeley. We thank Professor Jeffrey R. Long for samples of MOFs.

**Keywords:** ab initio calculations · iron · isomerization · photochemistry · ruthenium

- [1] For a perspective, see: a) I. Gur, K. Sawyer, R. Prasher, *Science* **2012**, *335*, 1454; for a review, see: b) T. J. Kucharski, Y. Tian, S. Akbulatov, R. Boulatov, *Energy Environ. Sci.* **2011**, *4*, 4449; for very recent work, see, e.g., c) T. J. Kucharski, N. Ferralis, A. M. Kolpak, J. O. Zheng, D. G. Nocera, J. C. Grossman, *Nature Chem.* **2014**, *6*, 441; d) E. Durgun, J. C. Grossman, *J. Phys. Chem. Lett.* **2013**, *4*, 854; e) A. M. Kolpak, J. C. Grossman, *J. Chem. Phys.* **2013**, *138*, 034303.
- [2] a) K. Börjesson, A. Lennartson, K. Moth-Poulsen, *J. Fluorine Chem.* **2014**, *161*, 24; b) Z. Hou, S. C. Nguyen, J. P. Lomont, C. B. Harris, N. Vinokurov, K. P. C. Vollhardt, *Phys. Chem. Chem. Phys.* **2013**, *15*, 7466; c) K. Börjesson, D. Dzebo, B. Albinsson, K. Moth-Poulsen, *J. Mater. Chem. A* **2013**, *1*, 8521; d) K. Börjesson, A. Lennartson, K. Moth-Poulsen, *ACS Sustainable Chem. Eng.* **2013**, *1*, 585; e) K. Moth-Poulsen, D. Coso, K. Börjesson, N. Vinokurov, S. K. Meier, A. Majumdar, K. P. C. Vollhardt, R. A. Segalman, *Energy Environ. Sci.* **2012**, *5*, 8534; f) M. R. Harpham, S. C. Nguyen, Z. Hou, J. C. Grossman, C. B. Harris, M. W. Mara, A. B. Stickrath, Y. Kanai, A. M. Kolpak, D. Lee, D. Liu, J. P. Lomont, K. Moth-Poulsen, N. Vinokurov, L. X. Chen, K. P. C. Vollhardt, *Angew. Chem.* **2012**, *124*, 7812; *Angew. Chem. Int. Ed.* **2012**, *51*, 7692; g) J. Cho, L. Berbil-Bautista, I. V. Peche-nezhskiy, N. Levy, S. K. Meier, V. Srinivasan, Y. Kanai, J. C. Grossman, K. P. C. Vollhardt, M. F. Crommie, *ACS Nano* **2011**, *5*, 3701; h) Y. Kanai, V. Srinivasan, S. K. Meier, K. P. C. Vollhardt, J. C. Grossman, *Angew. Chem.* **2010**, *122*, 9110; *Angew. Chem. Int. Ed.* **2010**, *49*, 8926; i) B. Zhu, O. Š. Miljanić, K. P. C. Vollhardt, M. J. West, *Synthesis* **2005**, *19*, 3373; j) R. Boese, J. K. Cammack, A. J. Matzger, K. Pflug, W. B. Tolman, K. P. C. Vollhardt, T. W. Weidman, *J. Am. Chem. Soc.* **1997**, *119*, 6757; k) K. P. C. Vollhardt, T. W. Weidman, *J. Am. Chem. Soc.* **1983**, *105*, 1676.
- [3] J. P. Perdew, K. Burke, M. Ernzerhof, *Phys. Rev. Lett.* **1996**, *77*, 3865.
- [4] For the “fulvalene effect”, see: a) C. G. de Azevedo, K. P. C. Vollhardt, *Synlett* **2002**, *34*, 1019; b) M. Tilstet, K. P. C. Vollhardt, R. Boese, *Organometallics* **1994**, *13*, 3146; c) P. A. McGovern, K. P. C. Vollhardt, *Synlett* **1990**, *9*, 493; see also: d) P. Aguirre-Etcheverry, D. O'Hare, *Chem. Rev.* **2010**, *110*, 4839; e) M. González-Maupoe, V. Tabernero, T. Cuenca, *Coord. Chem. Rev.* **2009**, *253*, 1854; f) A. Ceccon, S. Santi, L. Orian, A. Bissello, *Coord. Chem. Rev.* **2004**, *248*, 683.
- [5] For the effect of polar groups on the strength of the metal-carbon bond, see, for example: a) Y. Jiao, J. Morris, W. W. Brennessel, W. D. Jones, *J. Am. Chem. Soc.* **2013**, *135*, 16198; b) D. H. Ess, T. B. Gunnoe, T. R. Cundari, W. A. Goddard III, R. A. Periana, *Organometallics* **2010**, *29*, 6801; c) M. E. Evans, T. Li, A. J. Vetter, R. D. Rieth, W. D. Jones, *J. Org. Chem.* **2009**, *74*, 6907; d) E. Clot, C. Mégret, O. Eisenstein, R. N. Perutz, *J. Am. Chem. Soc.* **2009**, *131*, 7817; for a review, see: e) J. A. M. Simoes, J. L. Beauchamp, *Chem. Rev.* **1990**, *90*, 629.
- [6] There is tenuous (occasionally contradictory) evidence for M–M bond weakening when replacing L=CO with L=donor, often ascribed (L=PR<sub>3</sub>) to steric effects. See, for example: a) S. Trupia, T. E. Bitterwolf, W. E. Geiger, *Organometallics* **2012**, *31*, 6063; b) R. J. Klingler, M. J. Chen, J. W. Rathke, K. W. Kramarz, *Organometallics* **2007**, *26*, 352; c) T. S. Chong, P. Li, W. K. Leong, W. Y. Fan, *J. Organomet. Chem.* **2005**, *690*, 4132; d) G. Jansen, M. Schubart, B. Findeis, L. H. Gade, I. J. Scowen, M. McPartlin, *J. Am. Chem. Soc.* **1998**, *120*, 7239; e) K. Nunokawa, S. Onaka, T. Yamaguchi, M. Yaguchi, T. Tatematsu, S. Watase, M. Nakamoto, T. Ito, *J. Coord. Chem.* **2002**, *55*, 1353; f) K. R. Pope, M. S. Wrighton, *J. Am. Chem. Soc.* **1987**, *109*, 4545; g) A. J. Poe, R. A. Jackson, *Inorg. Chem.* **1978**, *17*, 2330; h) D. M. Chowdhury, A. Poë, K. R. Sharma, *J. Chem. Soc. Dalton Trans.* **1977**, 2352; i) J. P. Fawcett, A. Poë, *J. Chem. Soc. Dalton Trans.* **1977**, 1302; j) J. P. Fawcett, A. J. Poë, M. V. Twigg, *J. Chem. Soc. Chem. Commun.* **1973**, 267; k) C. E. Coffey, J. Lewis, R. S. Nyholm, *J. Chem. Soc.* **1964**, 1741.
- [7] Taking 3,4-di-*tert*-butylpyrrole as a model and a conservative estimate of its strain energy of 10.1 kcal mol<sup>-1</sup>: a) E. H. Wiebenga, E. Bouwhuis, *Tetrahedron* **1969**, *25*, 453; a later computation arrives at 15.7 kcal mol<sup>-1</sup>: b) J. Nakayama, Y. Sugihara, K. Terada, *Tetrahedron Lett.* **1990**, *31*, 4473.
- [8] a) E. L. Eliel, S. H. Wilen, L. N. Mander, *Stereochemistry of Organic Compounds*, Wiley, Hoboken, **1994**, pp. 696–697; ferrocenylcyclohexane: b) H. Falk, H. Lehner, K. Schlögl, *J. Organomet. Chem.* **1973**, *55*, 191.
- [9] a) S.-Z. Hu, Z.-H. Zhou, B. E. Robertson, *Z. Kristallogr.* **2009**, *224*, 375; b) A. Bondi, *J. Phys. Chem.* **1964**, *68*, 441.
- [10] R. Brand, H.-P. Krimmer, H.-J. Lindner, V. Sturm, K. Hafner, *Tetrahedron Lett.* **1982**, *23*, 5131.
- [11] a) F. Nief, L. Ricard, *J. Organomet. Chem.* **1998**, *553*, 503; b) P. Jutzi, J. Schnittger, W. Wieland, B. Neumann, H.-G. Stammler, *J. Organomet. Chem.* **1991**, *415*, 425; c) P. Jutzi, J. Schnittger, J. Dahlhaus, D. Gestmann, H.-C. Leue, *J. Organomet. Chem.* **1991**, *415*, 117; d) P. Jutzi, J. Schnittger, M. B. Hursthouse, *Chem. Ber.* **1991**, *124*, 1693; e) P. Jutzi, J. Schnittger, B. Neumann, H.-G. Stammler, *J. Organomet. Chem.* **1991**, *410*, C13; f) P. Jutzi, J. Schnittger, *Chem. Ber.* **1989**, *122*, 629.
- [12] For related iodine-bridged CpRu dimers, see: a) E. A. Nyawade, H. B. Friedrich, C. M. M'thuruaine, B. Omondi, *J. Mol. Struct.* **2013**, *1048*, 426; b) B. Schneider, I. Goldberg, D. Reshef, Z. Stein, Y. Shvo, *J. Organomet. Chem.* **1999**, *588*, 92; c) J. A. Cabeza, C. Landázuri, L. A. Oro, D. Belletti, A. Tiripicchio, M. Tiripicchio Camellini, *J. Chem. Soc. Dalton Trans.* **1989**, 1093; d) R. J. Haines, A. L. du Preez, *J. Chem. Soc. Dalton Trans.* **1972**, 944.
- [13] a) S. Müller, M. J. Webber, B. List, *J. Am. Chem. Soc.* **2011**, *133*, 18534; b) F. Zhanga, Y. Mu, L. Zhao, Y. Zhang, W. Bu, C. Chen, H. Zhai, H. Hong, *J. Organomet. Chem.* **2000**, *613*, 68; c) T. A. Geissman, C. F. Koelsch, *J. Org. Chem.* **1938**, *3*, 489.
- [14] For a review of sterically hindered organometallics, see: S. Brydges, L. E. Harrington, M. J. McGlinchey, *Coord. Chem. Rev.* **2002**, *233–234*, 75.
- [15] A. Gilbert, in *CRC Handbook of Organic Photochemistry and Photobiology* (Eds.: W. Horspool, F. Lenci), 2nd ed edCRC, Boca Raton, **2004**, 33/1–33/11.
- [16] a) A. Bauer, H. Hilbig, W. Hiller, E. Hinterschwepfinger, F. H. Köhler, M. Neumayer, *Synthesis* **2001**, 0778; b) M. L. Marcos, C. Moreno, R. M. Medina, M.-J. Macazaga, S. Delgado, J. González-Velasco, *J. Organomet. Chem.* **1998**, *568*, 185; c) T. Hirao, M. Kurashina, K. Aramaki, H. Nishihara, *J. Chem. Soc. Dalton Trans.* **1996**, 2929; d) S. Delgado, M. J. Macazaga, R. M. Medina, C. Moreno, J. González-Velasco, M. L. Marcos, D. H. Farrar, R. Ramachandran, *Organometallics* **1996**, *15*, 5416.

- [17] See, e.g.: a) P. Johnston, M. S. Loonat, W. L. Ingham, L. Carlton, N. J. Coville, *Organometallics* **1987**, *6*, 2121; b) D. J. Meyerhoff, R. Nunlist, M. Tilset, K. P. C. Vollhardt, *Magn. Reson. Chem.* **1986**, *24*, 709.
- [18] R. Boese, R. L. Myrabo, D. A. Newman, K. P. C. Vollhardt, *Angew. Chem.* **1990**, *102*, 589; *Angew. Chem. Int. Ed. Engl.* **1990**, *29*, 549.
- [19] B. Li, X. Tan, S. Xu, H. Song, B. Wang, *J. Organomet. Chem.* **2009**, *694*, 1503.
- [20] For recent discussions of the subject, see: a) J. E. Coughlin, Z. B. Henson, G. C. Welch, G. C. Bazan, *Acc. Chem. Res.* **2014**, *47*, 257; b) L.-L. Li, E. W.-G. Diau, *Chem. Soc. Rev.* **2013**, *42*, 291.
- [21] a) V. Cadierno, J. Díez, M. P. Gamasa, J. Gimeno, E. Lastra, *Coord. Chem. Rev.* **1999**, *193–195*, 147; b) M. J. Calhorda, L. F. Veiros, *Coord. Chem. Rev.* **1999**, *185–186*, 37.
- [22] K. A. Ingersoll, *Appl. Opt.* **1971**, *10*, 2781.
- [23] The unlinked Cp analogue Cp<sub>2</sub>FeRu(CO)<sub>4</sub> (which contains bridging carbonyls) is known: a) B. P. Gracey, S. A. R. Knox, K. A. MacPherson, A. G. Orpen, *J. Organomet. Chem.* **1984**, *272*, C45; b) H. R. Allcock, L. J. Wagner, M. L. Levin, *J. Am. Chem. Soc.* **1983**, *105*, 1321.
- [24] a) R. F. Bryan, P. T. Greene, *J. Chem. Soc. A* **1970**, 3064; b) O. S. Mills, *Acta Crystallogr.* **1958**, *11*, 620.
- [25] a) J. T. Mague, *Acta Crystallogr. Sect. C* **1995**, *51*, 831; b) O. S. Mills, P. J. P. Nice, *J. Organomet. Chem.* **1967**, *9*, 339.
- [26] K. P. C. Vollhardt, T. W. Weidman, *Organometallics* **1984**, *3*, 82.
- [27] J. C. Smart, C. J. Curtis, *Inorg. Chem.* **1977**, *16*, 1788.
- [28] H. B. Abrahamson, M. J. Heeg, *Inorg. Chem.* **1984**, *23*, 2281.
- [29] J. S. Drage, K. P. C. Vollhardt, *Organometallics* **1986**, *5*, 280.
- [30] P. A. McGovern, K. P. C. Vollhardt, *Chem. Commun.* **1996**, 1593.
- [31] M. L. Linares, N. Sánchez, R. Alajarin, J. J. Vaquero, J. Alvarez-Builla, *Synthesis* **2001**, 0382.
- [32] Prepared following: a) E. Le Carre, N. Lewis, C. Ribas, A. Wells, *Org. Process Res. Dev.* **2000**, *4*, 606; b) B. L. Feringa, B. de Lange, W. F. Jager, E. P. Schudde, *J. Chem. Soc. Chem. Commun.* **1990**, 804.
- [33] S. H. Hosseini, *J. Appl. Polym. Sci.* **2006**, *101*, 3920.
- [34] a) A. L. Tchougréeff, A. M. Tokmachev, R. Dronskowski, *Int. J. Quantum Chem.* **2013**, *113*, 1833; b) T. E. Shubina, T. Clark, *Z. Naturforsch. B* **2010**, *65*, 347; c) J.-J. Zou, M.-Y. Zhang, B. Zhu, L. Wang, X. Zhang, Z. Mi, *Catal. Lett.* **2008**, *124*, 139; d) L. Gu, F. Liu, *React. Kinet. Catal. Lett.* **2008**, *95*, 143; e) H.-F. Fan, C.-Y. Chang, T.-L. Chin, T.-I. Ho, K.-C. Lin, *J. Phys. Chem. B* **2006**, *110*, 5563; f) H.-F. Fan, T.-L. Chin, K.-C. Lin, *J. Phys. Chem. B* **2004**, *108*, 9364; g) A. D. Dubonosov, V. A. Bren, V. A. Chernoiyanov, *Russ. Chem. Rev.* **2002**, *71*, 917; h) R. Herges, F. Starck, T. Winkler, M. Schmittel, *Chem. Eur. J.* **1999**, *5*, 2965; i) R. D. Bach, I. L. Schilke, H. B. Schlegel, *J. Org. Chem.* **1996**, *61*, 4845; j) M. Kajitani, T. Fujita, T. Okumachi, M. Yokoyama, H. Hatano, H. Ushijima, T. Akiyama, A. Sugimori, *J. Mol. Catal.* **1992**, *77*, L1; k) A. Yamashita, K. Hasebe, K.-I. Hirao, *Chem. Lett.* **1992**, 1481; l) V. A. Bren, A. D. Dubonosov, V. I. Minkin, V. A. Chernoiyanov, *Russ. Chem. Rev.* **1991**, *60*, 451, and references therein.
- [35] R. Moulton, T. W. Weidman, K. P. C. Vollhardt, A. J. Bard, *Inorg. Chem.* **1986**, *25*, 1846.
- [36] a) C. H. Ko, H.-I. Song, J.-H. Park, S.-S. Han, J.-N. Kim, *Korean J. Chem. Eng.* **2007**, *24*, 1124; b) adapted from: T.-S. Li, J.-T. Li, H.-Z. Li, *J. Chromatogr. A* **1995**, *715*, 372.
- [37] K. P. C. Vollhardt, T. W. Weidman, unpublished results.
- [38] G. Lapisardi, F. Chiker, F. Launay, J. P. Nogier, J. L. Bonardet, *Catal. Commun.* **2004**, *5*, 277.
- [39] K. Bachari, O. Cherifi, *J. Mol. Catal. A* **2006**, *260*, 19.
- [40] C. N. Rhodes, D. R. Brown, *J. Chem. Soc. Faraday Trans.* **1993**, *89*, 1387.
- [41] R. Aigner, H. Spitz, R. W. Frei, *Anal. Chem.* **1976**, *48*, 2.
- [42] K. C. Vrancken, P. van der Voort, K. Possemiers, E. F. Vansant, *J. Colloid Interface Sci.* **1995**, *174*, 86.
- [43] Made in analogy to: S. I. Mostafa, S. Ikeda, B. Ohtani, *J. Mol. Catal. A* **2005**, *225*, 181.
- [44] a) M. Machida, B. Fotoohia, Y. Amamo, T. Ohba, H. Kanoh, L. Mercier, *J. Hazard. Mater.* **2012**, *221–222*, 220; b) J. Tang, L. Wang, G. Liu, Y. Liu, Y. Hou, W. Zhang, M. Jia, W. R. Thiel, *J. Mol. Catal. A* **2009**, *313*, 31; c) K. Miki, Y. Sato, *Bull. Chem. Soc. Jpn.* **1993**, *66*, 2385.
- [45] W. B. Schaap, D. L. McMasters, *J. Am. Chem. Soc.* **1961**, *83*, 4699.
- [46] Z. R. Herm, J. A. Swisher, B. Smit, R. Krishna, J. R. Long, *J. Am. Chem. Soc.* **2011**, *133*, 5664.
- [47] K. Sumida, S. Horike, S. S. Kaye, Z. R. Herm, W. L. Queen, C. M. Brown, F. Grandjean, G. J. Long, A. Dailly, J. R. Long, *Chem. Sci.* **2010**, *1*, 184.
- [48] See, e.g.: L. A. Tyler, J. C. Noveron, M. M. Olmstead, P. K. Mascharak, *Inorg. Chem.* **2000**, *39*, 357.
- [49] For selected reviews, see: a) C. B. Brochini, J. H. G. Lago, *Braz. J. Pharmacogn.* **2007**, *17*, 266; b) O. K. Guha, J. Janák, *J. Chromatogr.* **1972**, *68*, 325; c) F. B. Padley, *Chromatogr. Rev.* **1966**, *8*, 208; see also: J. T. Dillon, Y. Huang, Abstracts of Papers, 247th ACS National Meeting & Exposition, Dallas, TX, USA, March 16–20, 2014, ANYL-160.
- [50] See, for example: a) F.-H. Du, K.-X. Wang, W. Fu, P.-F. Gao, J.-F. Wang, J. Yang, J.-S. Chen, *J. Mater. Chem. A* **2013**, *1*, 13648; b) X. Wang, X. Liu, X. Wang, *J. Mol. Struct.* **2011**, *997*, 64; c) C. Weiping, Z. Lide, *J. Phys. Condens. Matter* **1997**, *9*, 7257.
- [51] See also: K. M. Rourke, C. Nataro, *J. Organomet. Chem.* **2002**, *656*, 181.
- [52] N. G. Connelly, W. G. Geiger, *Chem. Rev.* **1996**, *96*, 877.
- [53] SMART: Area-Detector Software Package, Bruker Analytical X-ray Systems Inc., Madison, WI, **1995–1999**.
- [54] SAINT: SAX Area-Detector Integration Program, V. 7.06, Siemens Industrial Automation Inc., Madison, WI, **2005**.
- [55] XPREP: SHELXTL Crystal Structure Determination Package, V. 6.12, Bruker AXS Inc., Madison, WI, **1995**.
- [56] SADABS: Siemens Area Detector ABSorption Correction Program, V. 2.10, George Sheldrick, **2005**.
- [57] XS: Program for the Solution of X-ray Crystal Structures, SHELXTL Crystal Structure Determination Package, Bruker Analytical X-ray Systems Inc., Madison, WI, **1995–1999**.
- [58] XL: Program for the Refinement of X-ray Crystal Structures, SHELXTL Crystal Structure Determination Package, Bruker Analytical X-ray Systems Inc., Madison, WI, **1995–1999**.

Received: June 29, 2014

Published online on October 3, 2014